

# Electron-Density Profiles of the Ionosphere Observed Near Washington, D.C., During the Spring of 1971

J. M. GOODMAN, M. W. LEHMAN, E. L. GOTT,  
K. W. MORIN, AND E. PIERNIK

*Radar Geophysics Branch  
Radar Division*

June 7, 1972



**NAVAL RESEARCH LABORATORY**  
Washington, D.C.

Approved for public release; distribution unlimited.

## DOCUMENT CONTROL DATA - R &amp; D

*(Security classification of title, body of abstract and indexing annotation must be entered when the overall report is classified)*

1. ORIGINATING ACTIVITY (Corporate author) Naval Research Laboratory Washington, D.C. 20390		2a. REPORT SECURITY CLASSIFICATION Unclassified	
		2b. GROUP	
3. REPORT TITLE ELECTRON-DENSITY PROFILES OF THE IONOSPHERE OBSERVED NEAR WASHINGTON, D.C., DURING THE SPRING OF 1971			
4. DESCRIPTIVE NOTES (Type of report and inclusive dates) A final report on one phase of the problem; work on other phases continues.			
5. AUTHOR(S) (First name, middle initial, last name) John M. Goodman, Melvin W. Lehman, Edgar L. Gott, Kenneth W. Morin, Edward Piernik			
6. REPORT DATE June 7, 1972		7a. TOTAL NO. OF PAGES 40	7b. NO. OF REFS 13
8a. CONTRACT OR GRANT NO. NRL Problem R07-28		9a. ORIGINATOR'S REPORT NUMBER(S) NRL Report 7395	
b. PROJECT NO. RR 008-01-41-5557		9b. OTHER REPORT NO(S) (Any other numbers that may be assigned this report)	
c.			
d.			
10. DISTRIBUTION STATEMENT Approved for public release; distribution unlimited.			
11. SUPPLEMENTARY NOTES		12. SPONSORING MILITARY ACTIVITY Department of the Navy Office of Naval Research Arlington, Virginia 22217	
13. ABSTRACT  Radar Thomson scatter observations of the midday ionosphere over Randle Cliff have been made during March-May 1971. The correlation between various ionospheric parameters has been determined. Emphasis has been placed on the effect that magnetic activity has on the shape of the electron-density distribution. In general, following a magnetic impulse, the F2 maximum height is initially raised in proportion to the amount of magnetic activity, is subsequently lowered, and eventually returns to the equilibrium position. Also the F2 maximum density and the total electron content (below 600 km) decrease as the length of time between the magnetic-activity impulse and the measurement increases. This situation exists for at least a day; thereafter the diminution is reduced, and the profile gradually assumes its average shape.			

14. KEY WORDS	LINK A		LINK B		LINK C	
	ROLE	WT	ROLE	WT	ROLE	WT
Thomson scatter Faraday rotation Electron content Electron density Slab thickness Magnetic activity						

## CONTENTS

Abstract .....	ii
Problem Status .....	ii
Authorization .....	ii
INTRODUCTION .....	1
MEASUREMENTS .....	1
Composite Profiles for March, April, and May .....	1
Ionospheric Parameters .....	3
Crosscorrelation of the Ionospheric Parameters .....	5
MODIFICATION OF IONOSPHERIC PARAMETERS BY MAGNETIC ACTIVITY .....	6
Translation of the Coefficient of Correlation to the Fractional Change in the Ionospheric Parameter .....	13
ILLUSTRATION OF MAGNETIC-ACTIVITY RESPONSE .....	14
DISCUSSION .....	19
SUMMARY .....	21
REFERENCES .....	21
APPENDIX—Electron-Density Distributions for March, April, and May 1971 .....	23

## ABSTRACT

Radar Thomson scatter observations of the midday ionosphere over Randle Cliff have been made during March-May 1971. The correlation between various ionospheric parameters has been determined. Emphasis has been placed on the effect that magnetic activity has on the shape of the electron-density distribution. In general, following a magnetic impulse, the F2 maximum height is initially raised in proportion to the amount of magnetic activity, is subsequently lowered, and eventually returns to the equilibrium position. Also the F2 maximum density and the total electron content (below 600 km) decrease as the length of time between the magnetic-activity impulse and the measurement increases. This situation exists for at least a day; thereafter the diminution is reduced, and the profile gradually assumes its average shape.

## PROBLEM STATUS

A final report on one phase of the problem. Work continues on other phases.

## AUTHORIZATION

NRL Problem R07-28  
Project RR 008-01-41-5557

Manuscript submitted January 25, 1972.

# ELECTRON-DENSITY PROFILES OF THE IONOSPHERE OBSERVED NEAR WASHINGTON, D.C., DURING THE SPRING OF 1971

## INTRODUCTION

This report describes the results of radar Thomson scatter observations made in March, April, and May 1971. An interim report outlining the March results has been published (1). The ionospheric response to magnetic activity was of particular interest, and this topic will receive considerably more attention in this report. The experimental configuration and the data-analysis techniques employed in the determination of the electron-density profiles presented here have been reported earlier (1,2) and will not be repeated.

The principal results discussed in this report have been presented at the Fall meeting of the American Geophysical Union, and all of the profiles have been made available to interested scientists through the facilities of the World Data Center (3).

## MEASUREMENTS

A significant modification has been made in the method of computing electron-density profiles since the publication of the March results. Instead of assuming a constant value for the M factor ( $M = H \cos \theta \sec \chi$ ), its full altitude dependence has been incorporated into the computer program. This modification eliminates a systematic error of as much as 15% in the profiles.

Also, each of the nineteen March profiles were separately fitted to a fourth-degree least-squares polynomial to deduce the various ionospheric parameters. In this report profiles were obtained by combining the data corresponding to the same day of observation prior to determination of the polynomial. In addition the peak F-region density ( $N_{F2max}$ ) for each day has been taken to be the figure dictated by the polynomial rather than the maximum value associated with the set of unsmoothed raw estimates of density. This appears to bring the value of  $N_{F2max}$  more in line with the Wallops Island ionosonde results.

### Composite Profiles for March, April, and May

Figure 1 is a scatter plot of data obtained during March, April, and May 1971. A least-squares fourth-degree-polynomial fit to the raw data points is plotted. The decrease in  $N_{F2max}$  between March and May is seen quite clearly. This would be expected if past measurements of total content are used as a gauge, for it is well known that the total content is greater at the equinox than during the summer. Note that the data points in Fig. 1 appear to have preferred locations in some instances. This is not a real effect; rather it is a result of the analysis procedure which allows only quantum jumps in the Faraday rotational derivative. This has been discussed in an earlier report (1).

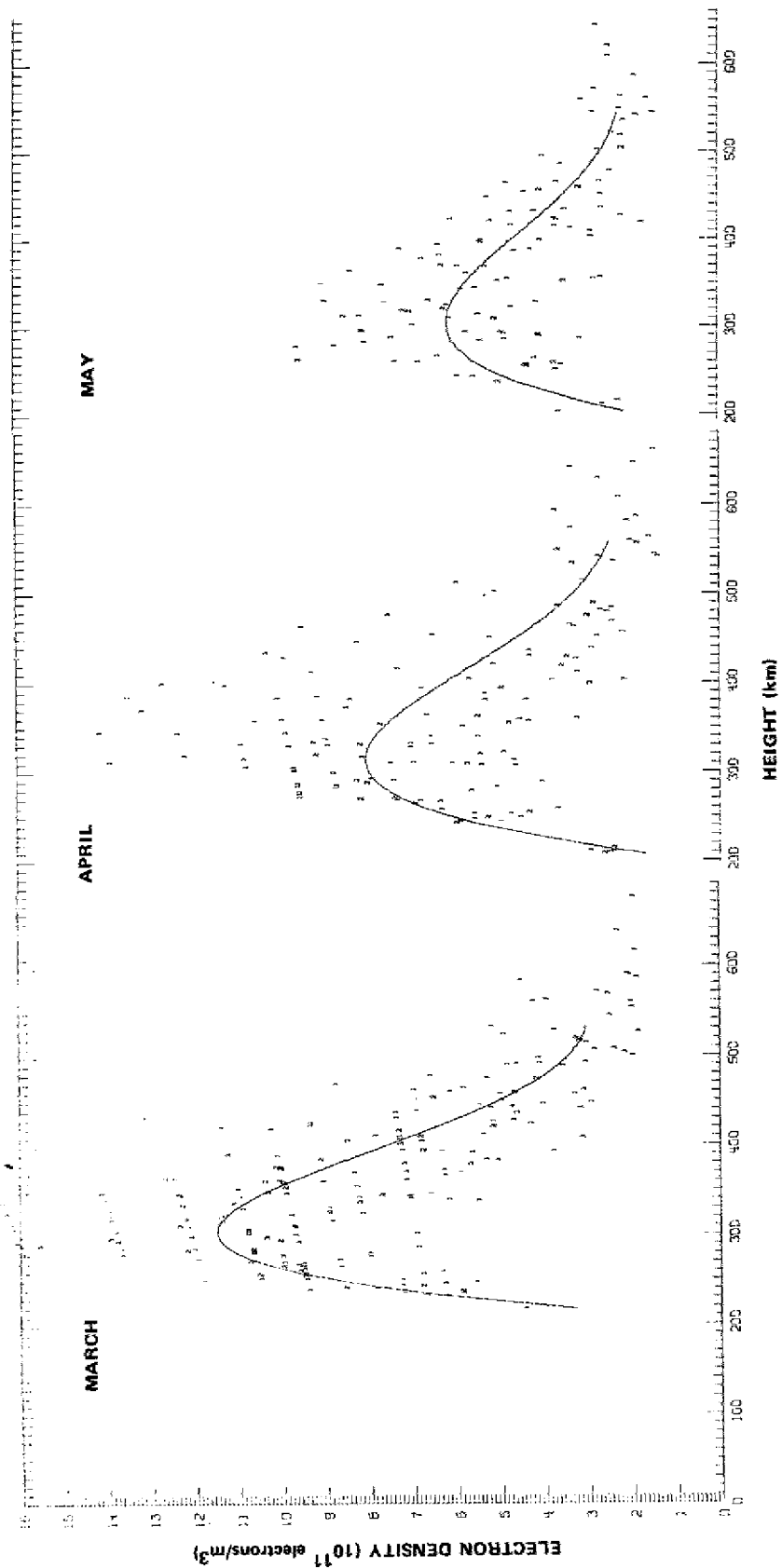


Fig. 1—Composite electron-density profiles for March, April, and May 1971. The March profile is based on ten days of operation; the April and May profiles each are based on eight days of operation.

Table 1 lists the days and times corresponding to the individual profiles on which the curves in Fig. 1 are based. The March profile is based on ten days of observation, and the April and May profiles are based on eight days of observation. The daily profiles are given in Appendix A.

Table 1  
Days and Times for the Profiles of Fig. 1

March 1971		April 1971		May 1971	
Day	Time (EST)	Day	Time (EST)	Day	Time (EST)
12	1346	21	1418	11	1450
12	1408	21	1444	11	1500
15	1450	22	1406	12	1353
15	1502	22	1418	12	1353
16	1337	23	1411	13	1418
16	1403	23	1425	13	1450
17	1310	26	1408	14	1440
17	1321	26	1418	14	1452
18	1334	27	1314	17	1451
18	1415	27	1345	17	1515
19	1320	28	1402	19	1338
19	1335	28	1434	19	1400
22	1320	29	1355	20	1502
22	1347	29	1438	20	1516
23	1607	30	1334	21	1330
		30	1345	21	1339
24	1539				
24	1551				
25	1503				
25	1518				

### Ionospheric Parameters

Parameters which have been deduced include the F2-maximum density ( $N_{F2max}$ ), the altitude of the F2 maximum ( $h_{F2max}$ ), the electron content to an altitude of 600 km [ $C(600)$ ], and the slab thickness to an altitude of 600 km [ $\tau(600)$ ]. These parameters are given in Table 2 for each day of operation, and the average values and standard deviations are given in Table 3. The upper limit for the computation of both slab thickness and content is dictated by the rapid diminution of Faraday rotation with height above the F2 maximum.

The practical upper limit was  $\approx 600$  km; this value was used for convenience and consistency, as a termination height in the analysis.

Table 2  
Atmospheric Parameters

Date (1971)	$N_{F2max}$ ( $10^{11}$ electrons/ $m^3$ )	$h_{F2max}$ (km)	C(600) ( $10^{17}$ electrons/ $m^2$ )	$\tau(600)$ (km)
March 12	13.88	310	3.23	232
15	11.65	290	2.45	210
16	10.92	280	2.41	221
17	12.00	310	2.82	235
18	8.78	300	2.17	248
19	13.76	320	3.23	235
22	13.04	290	2.77	212
23	13.67	300	2.85	208
24	9.23	310	2.28	247
25	8.22	290	1.83	222
April 21	11.81	340	2.99	254
22	7.80	290	1.80	230
23	4.57	310	1.35	296
26	9.25	310	2.26	245
27	9.06	290	1.95	216
28	6.30	300	1.48	235
29	7.16	300	1.83	256
30	7.15	280	1.71	239
May 11	5.23	300	1.39	265
12	8.39	310	2.26	280
13	4.86	320	1.47	302
14	5.85	350	1.80	308
17	5.62	360	1.18	210
19	5.44	300	1.43	264
20	6.89	300	1.80	262
21	7.04	280	1.85	263

Table 3  
Average Values (A) and Standard Deviations (S.D.) of the Ionospheric Parameters

Month and Year	Peak Electron Density ( $N_{F2max}$ )	F2 Maximum Height ( $h_{F2max}$ )	Electron Content to 600 km [C(600)]	Slab Thickness to 600 km [ $\tau(600)$ ]
March 1971	A = $11.52 \times 10^{11}/m^3$ S.D. = $2.51 \times 10^{11}/m^3$	A = 300 km S.D. = 2.47 km	A = $2.60 \times 10^{17}/m^2$ S.D. = $0.46 \times 10^{17}/m^2$	A = 227 km S.D. = 14.64 km
April 1971	A = $7.88 \times 10^{11}/m^3$ S.D. = $2.17 \times 10^{11}/m^3$	A = 302 km S.D. = 12.80 km	A = $1.92 \times 10^{17}/m^2$ S.D. = $0.51 \times 10^{17}/m^2$	A = 246 km S.D. = 23.87 km
May 1971	A = $6.15 \times 10^{11}/m^3$ S.D. = $1.18 \times 10^{11}/m^3$	A = 315 km S.D. = 27.25 km	A = $1.65 \times 10^{17}/m^2$ S.D. = $0.34 \times 10^{17}/m^2$	A = 269 km S.D. = 30.1 km

The average times corresponding to the Randle Cliff Radar (RCR) observations in March, April, and May were 1418, 1407, and 1427 EST respectively. Table 4 shows the average values of  $h_{F2max}$ ,  $N_{F2max}$ , and the total content below 600 km [C(600)] for the Randle Cliff Radar (RCR) site. For comparison, estimates of  $h_{F2max}$  and  $N_{F2max}$  have kindly been supplied by Dr. J. Nisbet\* of Pennsylvania State University on the basis of the CCIR† model. Also shown are the Wallops Island ionosonde values of  $N_{F2max}$ , which are based on 7-E form data supplied by Mr. R. Gray‡. The RCR values of  $N_{F2max}$  are somewhat higher than Nisbet's values for March and May but are lower in April. In addition the RCR values of  $h_{F2max}$  are consistently higher by  $\geq 20$  km than those obtained in the model. The Wallops Island values of  $N_{F2max}$  are in close agreement with the RCR observations, except during May when they differ by  $\approx 10\%$ . The percentage deviation is less than 1% in March and 2.8% in April.

Table 4  
Average Value of Ionospheric Parameters for the RCR Site

Parameter	Month and Year			Data Source
	March 1971	April 1971	May 1971	
$h_{F2max}(km)$	300 273	302 281	315 281	RCR Thomson Scatter Penn State Model
$N_{F2max}(m^{-3})$	$11.52 \times 10^{11}$ 8.31 11.49	$7.88 \times 10^{11}$ 8.22 7.66	$6.15 \times 10^{11}$ 5.50 5.50	RCR Thomson Scatter Penn State Model Wallops Island*
Total Content ( $m^{-2}$ )	$2.60 \times 10^{17}$ 2.29	$1.92 \times 10^{17}$ 2.48	$1.65 \times 10^{17}$ 1.78	RCR Thomson Scatter Penn State Model

\*Wallops Island data are based on hourly 7E-form data at 1400 EST. These data are said to be more accurate than the F-plot data.

### Crosscorrelation of the Ionospheric Parameters

Table 5 shows how the parameters  $N_{F2max}$ ,  $h_{F2max}$ , C(600), and  $\tau(600)$  are correlated during March, April, and May respectively. The behavior during March and April is quite similar, but the May behavior is considerably different. During March and April, fluctuations in the F2 maximum height are positively correlated with  $N_{F2max}$ , C(600), and  $\tau(600)$ , but these fluctuations are negatively correlated with the same parameters during May. Though the correlation between  $N_{F2max}$  and  $\tau(600)$  is negative during the first two months, there is no correlation between these two parameters during May. Also there is little correlation between C(600) and  $\tau(600)$  during March and April, but during May the correlation is significant (+0.41). The only consistent correlation is that linking the total content and

\*Private communication.

†Comite Consultatif International des Radiocommunications.

‡Private communication.

the F2 maximum density. The correlation was observed to be positive in all three cases, being +0.85 in March, +0.84 in April, and +0.77 in May. Thus, as expected,  $N_{F2max}$  strongly controls the total content. The exact cause for the difference between the combined March-April behavior and that for May is not known at present, but it is felt that the following facts may be significant:

- The peak electron density and total content for May were lower than for the two previous months.
- The monthly average 3-hourly Fredericksburg K index,  $K_{FR}$ , over a 24-hr period preceding the median observation time was found to be 1.80 in March, 2.12 in April, and 2.05 in May. However, K indices are roughly logarithmically related to magnetic activity. Since a minor geomagnetic storm occurred in May (and not in March or April), one finds that the actual magnetic activity, in terms of  $r^*$ , is greater in May than in either of the other two months.

Table 5  
Crosscorrelation of the Ionospheric Parameters

Month/Parameter	$\tau(600)$	C(600)	$h_{F2max}$
March } $N_{F2max}$	-0.37	+0.85	+0.29
April } $N_{F2max}$	-0.37	+0.84	+0.44
May } $N_{F2max}$	-0.01	+0.77	-0.27
March } $h_{F2max}$	+0.54	+0.51	
April } $h_{F2max}$	+0.40	+0.60	
May } $h_{F2max}$	-0.11	-0.29	
March } C(600)	-0.07		
April } C(600)	-0.14		
May } C(600)	+0.41		

#### MODIFICATION OF IONOSPHERIC PARAMETERS BY MAGNETIC ACTIVITY

To determine the relationships, if any, between magnetic activity and the parameters  $N_{F2max}$ ,  $h_{F2max}$ ,  $\tau(600)$ , and C(600), a crosscorrelation function was constructed between these parameters and  $K_{FR}$ . Tables 6, 7, and 8 list the lag intervals, the times to which they correspond, and the associated K indices† for March, April, and May respectively. The equivalent  $r$  values are also given.‡

\*The parameter  $r$  is a measure of the disturbance magnitude. At a magnetic latitude of 50 deg (close to the RCR latitude) the association to be made between K and  $r$  is approximately logarithmic, i.e.,  $K \approx a \log r$ . (See K. Davies, *Ionospheric Radio Propagation*, National Bureau of Standards, Monograph 80, GPO, Washington, D.C., 1965, pp. 26-25.)

†The listed values are actually sums of three adjacent  $K_{FR}$  indices (which are basically 3-hourly). These new indices will be symbolized by  $\Sigma K_{FR}$ . Each  $\Sigma K_{FR}$  index thus covers a 9-hr period of time, and every third index is completely independent.

‡The  $r$  values are based on the effective three-hourly average  $K_{FR}$ . That is, one finds the value of  $r$  corresponding to one third the tabulated value of  $\Sigma K_{FR}$ . The following correspondence is used:

$r$ :	0	5	10	20	40	70	120	200	330	500
$\Sigma K_{FR}/3$ :	0	1	2	3	4	5	6	7	8	9

and linear interpretation is used for values of  $\Sigma K_{FR}/3$  which fall between the tabular values.

Table 6  
March 1971 Magnetic Indices

Interval	Lag (hr)	Observation																			
		1		2		3		4		5		6		7		8		9		10	
		$\Sigma KFR$	r	$\Sigma KFR$	r	$\Sigma KFR$	r	$\Sigma KFR$	r	$\Sigma KFR$	r										
0	2.75	8	17	7	13	6	10	4	7	1	2	7	13	2	3	4	7	7	13	4	7
1	5.75	7	13	7	13	7	13	4	7	1	2	6	10	1	2	2	3	7	13	6	10
2	8.75	6	10	8	17	7	13	5	8	3	5	5	8	1	2	1	2	7	13	8	17
3	11.75	5	8	10	27	8	17	6	10	5	8	6	10	1	2	0	0	9	20	8	8
4	14.75	4	7	12	40	9	20	7	13	6	10	5	8	1	2	0	0	8	17	7	13
5	17.75	4	7	12	40	9	20	7	13	6	10	6	10	2	2	1	2	6	10	6	10
6	20.75	2	3	11	34	8	17	8	17	6	10	4	7	3	5	2	3	5	8	8	17
7	23.75	2	3	9	20	7	13	7	13	6	10	3	5	3	5	2	3	4	7	8	17
8	26.75	3	5	8	17	7	13	6	10	4	7	1	2	2	3	2	3	4	7	7	13
9	29.75	5	8	9	20	7	13	7	13	4	7	1	2	1	2	1	2	2	3	7	13
10	32.75	6	10	11	34	8	17	7	13	5	8	3	5	2	3	1	2	1	2	8	17
11	35.75	7	13	12	40	10	27	8	17	6	10	5	8	2	3	1	2	0	0	9	20
12	38.75	6	10	11	34	12	40	9	20	7	13	6	10	2	3	1	2	0	0	8	17
13	41.75	6	10	11	34	12	40	9	20	7	13	6	10	3	5	2	3	1	2	6	10
14	44.75	5	8	11	34	11	34	8	17	8	17	6	10	4	7	3	5	2	3	5	8

Table 7  
April 1971 Magnetic Indices

Internal	Lag (hr)	Observation															
		1		2		3		4		5		6		7		8	
		$\Sigma K_{FR}$	r														
0	2.75	8	17	6	10	5	8	6	10	4	7	10	27	6	10	3	5
1	5.75	7	13	5	8	5	8	4	7	5	8	11	34	6	10	4	7
2	8.75	7	13	7	13	6	10	3	5	7	13	10	27	6	10	6	10
3	11.75	5	8	8	17	7	13	1	2	8	17	9	20	7	13	8	17
4	14.75	2	3	10	27	5	8	1	2	7	13	9	20	8	17	10	27
5	17.75	1	2	11	34	6	10	0	0	6	10	8	17	8	17	11	34
6	20.75	4	7	12	40	7	13	1	2	6	10	7	13	7	13	10	27
7	23.75	5	8	10	27	7	13	1	2	6	10	5	8	8	17	8	17
8	26.75	5	8	8	17	6	10	1	2	6	10	4	7	10	27	6	10
9	29.75	3	5	7	13	5	8	1	2	4	7	5	8	11	34	6	10
10	32.75	4	7	7	13	7	13	2	3	3	5	7	13	10	27	6	10
11	35.75	5	8	5	8	8	17	2	3	3	5	8	17	9	20	7	13
12	38.75	5	8	2	3	10	27	1	2	1	2	7	13	9	20	8	17
13	41.75	5	8	1	2	11	34	0	0	0	0	6	10	8	17	8	17
14	44.75	5	8	4	7	12	40	0	0	1	2	6	10	7	13	7	13

Table 8  
May 1971 Magnetic Indices

Internal	Lag (hr)	Observation															
		1		2		3		4		5		6		7		8	
		$\Sigma K_{FR}$	r														
0	2.75	3	5	2	3	3	5	10	27	15	70	7	13	5	8	5	8
1	5.75	2	3	1	2	3	5	10	27	15	70	6	10	5	8	6	10
2	8.75	2	3	1	2	3	5	7	13	16	86	7	13	5	8	4	7
3	11.75	4	7	1	2	3	5	7	13	16	86	7	13	4	7	2	3
4	14.75	6	10	3	5	5	8	7	13	16	86	8	17	4	7	1	2
5	17.75	6	10	5	8	6	10	8	17	13	50	7	13	5	8	3	5
6	20.75	6	10	5	8	5	8	6	10	9	20	8	17	7	13	5	8
7	23.75	6	10	4	7	3	5	4	7	5	8	9	20	7	13	5	8
8	26.75	6	10	3	5	2	3	3	5	2	3	11	34	7	13	5	8
9	29.75	4	7	2	3	1	2	2	3	1	2	13	50	6	10	5	8
10	32.75	4	7	2	3	1	2	2	3	1	2	14	60	7	13	5	8
11	35.75	6	10	4	7	1	2	3	5	3	5	16	86	7	13	4	7
12	38.75	8	17	6	10	3	5	5	8	5	8	16	86	8	17	4	7
13	41.75	9	30	6	10	5	8	6	10	7	13	15	70	7	13	5	8
14	44.75	8	17	6	10	5	8	5	8	7	13	14	60	8	17	6	10

Functions which describe the time-varying correlation between the 3-hourly  $K_{FR}$  indices and the parameters  $N_{F2max}$ ,  $h_{F2max}$ ,  $C(600)$ , and  $\tau(600)$  are given in Figs. 2-4 corresponding to March, April, and May respectively. Prior to processing, the  $K_{FR}$  indices were smoothed by forming a running average of three consecutive three-hourly indices. Thus each value of  $K_{FR}$  used in the analysis, and tabulated in Tables 6-8, is actually characteristic of a 9-hr interval of time and is denoted by the symbol  $\Sigma K_{FR}$ . Nevertheless the spacing between the listings in Tables 6-8 is only 3 hr, since the basic  $K_{FR}$  data is 3-hourly. The lag associated with each 9-hr interval is actually the temporal midpoint of that interval; thus, for example, the so-called fifth lag interval, which extends between the lag times of 13.25 hr and 22.25 hr, is assigned a mean lag time of 17.75 hr. In addition the correlation coefficient between  $\Sigma K_{FR}$  and an ionospheric parameter for the fifth lag interval represents the ionospheric response to an impulse of magnetic activity which occurred 17.75 hr earlier on the average.

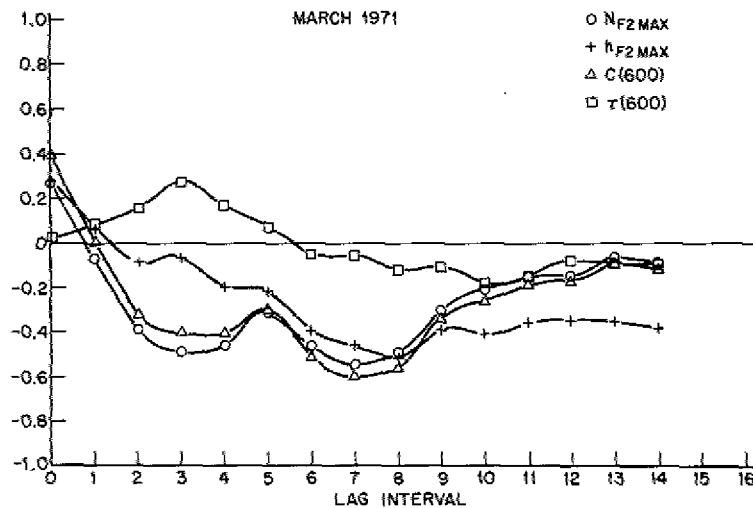


Fig. 2—Correlation functions relating the dependence of the ionospheric parameters on magnetic activity for March 1971

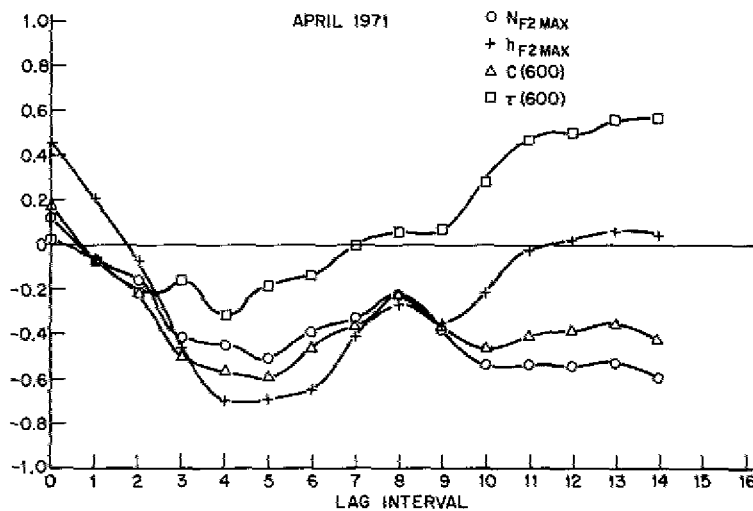


Fig. 3—Correlation functions relating the dependence of the ionospheric parameters on magnetic activity for April 1971

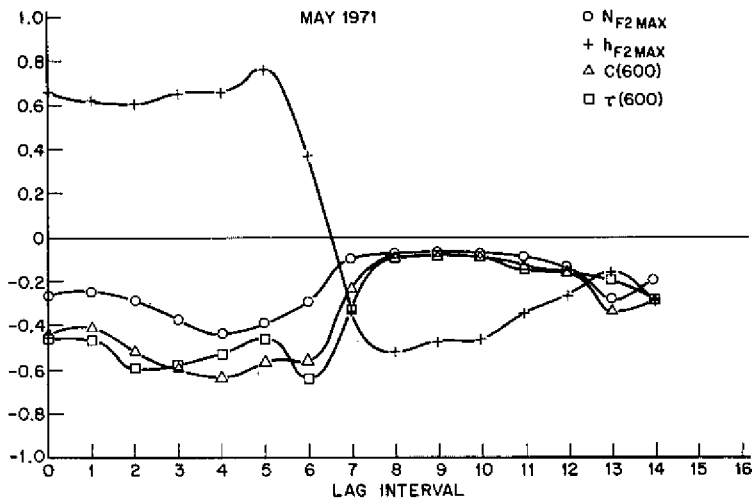


Fig. 4—Correlation functions relating the dependence of the ionospheric parameters on magnetic activity for May 1971

Assuming that a positive excursion in magnetic activity ( $+\delta\Sigma K_{FR}$ ) has occurred, then a positive correlation coefficient linking  $\Sigma K_{FR}$  and an ionospheric parameter  $P$  implies that the parameter will experience a positive excursion  $\delta P > 0$ , where  $\delta P$  is proportional to the magnitude of the correlation coefficient. If the correlation were negative, then a positive excursion ( $+\delta\Sigma K_{FR}$ ) implies a down ward excursion in the parameter  $\delta P < 0$ , where again  $\delta P$  is proportional to the magnitude of the correlation coefficient.

Fig. 5 was prepared to compare more readily on a monthly basis the effect of magnetic activity on a particular parameter, say  $N_{F2max}$ . The monthly comparisons for  $C(600)$ ,  $\tau(600)$ , and  $h_{F2max}$  are given in Figs. 6-8.

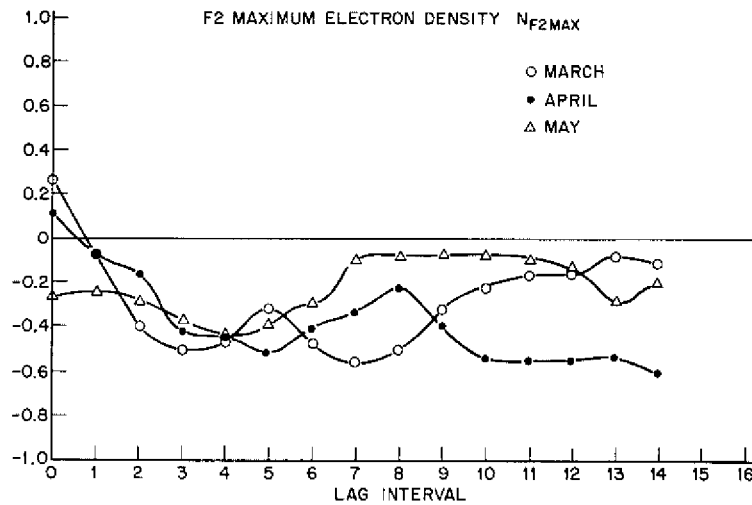


Fig. 5—Correlation functions relating the dependence of  $N_{F2max}$  magnetic activity for March, April, and May 1971

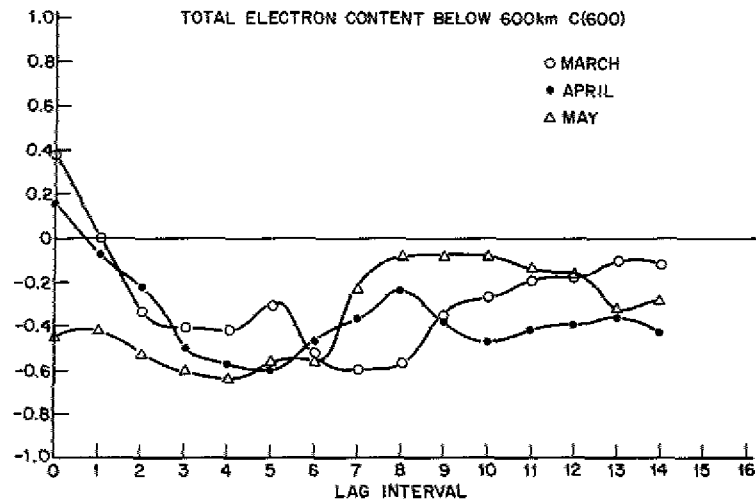


Fig. 6—Correlation functions relating the dependence of C(600) on magnetic activity for March, April, and May 1971

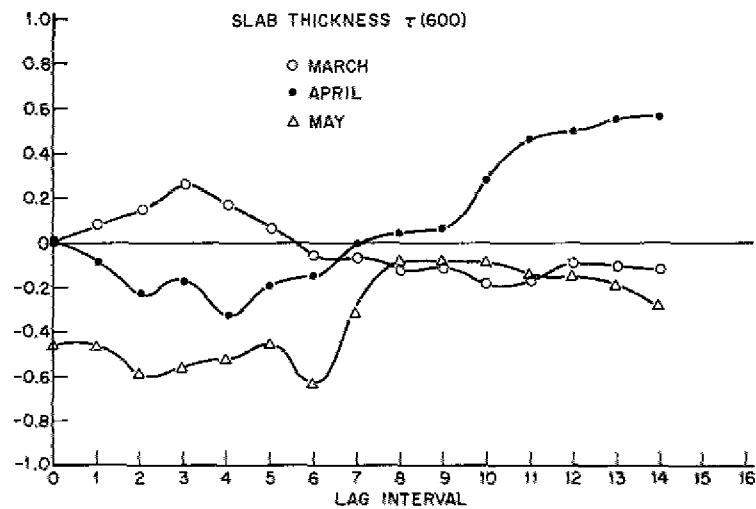


Fig. 7—Correlation functions relating the dependence of  $\tau$ (600) on magnetic activity for March, April, and May 1971

On inspection of Fig. 5, it is rather obvious that the F2 maximum electron density is negatively correlated with the magnetic activity. Generally speaking the correlation at small time lags is low but slightly positive during March and April and somewhat negative during May. At later times the correlation is again low during March and May but strongly negative during April. One consistent feature is that the correlation is rather strongly negative between lag intervals of 3 and 6 or for an average lag of  $\approx 16.25$  hr. Hence the phenomena which are responsible for the diminution of electron population near the F2 maximum are maximized at roughly 16 hr following an impulse of magnetic activity.

Since  $N_{F2max}$  and C(600) are highly correlated, it is not surprising that the same statements just made concerning  $N_{F2max}$  and  $\Sigma K_{FR}$  also hold the C(600) and  $\Sigma K_{FR}$ . One can notice the similarity of Figs. 5 and 6.

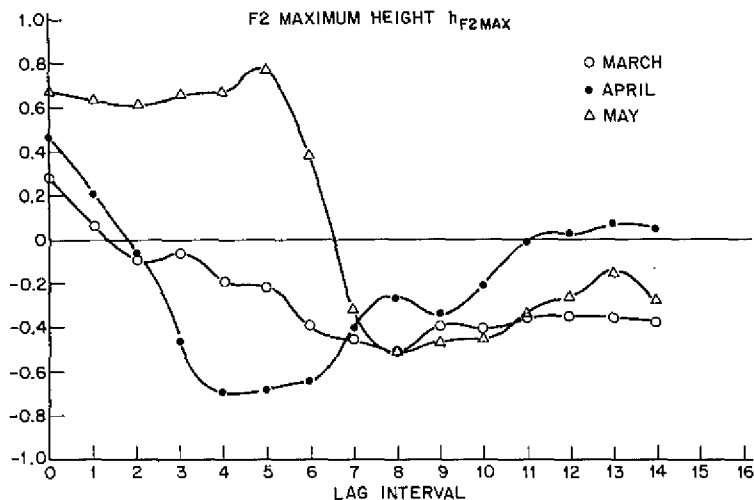


Fig. 8—Correlation functions relating the dependence of  $h_{F2max}$  magnetic activity for March, April, and May 1971

As seen in Fig. 8, the F2 maximum height  $h_{F2max}$  is generally positively correlated with  $\Sigma K_{FR}$  for small lag times. One can recall that the actual monthly magnetic activity, as indicated by the parameter  $r$ , satisfies the inequality  $\bar{r}_{May} > \bar{r}_{April} > \bar{r}_{March}$ , where the bar denotes the average. For the first two lag intervals, the degree of correlation between  $h_{F2max}$  and  $\Sigma K_{FR}$  ( $\rho(h_{F2max}, \Sigma K_{FR}, lag)$ ) exhibits the same monthly ordering, i.e.,  $\rho_{May} > \rho_{April} > \rho_{March}$ . Again, although the situation is not easy to generalize, the overall pattern could be described as follows: First, the F2 maximum height is raised in proportion to the amount of magnetic activity. Second, the F2 maximum descends below its equilibrium value; this condition occurs near the fifth lag interval ( $\approx 17.75$  hr) in April and near the eighth lag interval ( $\approx 26.75$  hr) in March and May. Finally, there is a tendency for the F2 maximum to return to its equilibrium position after a long time.

Figure 7 shows how the so-called slab thickness depends on the lag time for March, April, and May. In April and May the initial response is an increasing negative correlation between  $\tau$  and  $\Sigma K_{FR}$  with a tendency toward more positive correlation at later times. The situation is reversed in March.

#### Translation of the Coefficient of Correlation to the Fractional Change in the Ionospheric Parameter

The sample correlation coefficient  $\rho$  between two sets of data A and B is defined by

$$\rho(A, B) = \frac{1}{N\sigma_A\sigma_B} \sum_{i=1}^N (A_i - \bar{A})(B_i - \bar{B}) , \quad (1)$$

where  $\sigma_A$  and  $\sigma_B$  are the standard deviations of A and B and where  $\bar{A}$  and  $\bar{B}$  are the averages. Also if A and B are normally distributed variables, it is well known that the line of regression of A upon B is given by

$$A(B) = \rho(A, B) \frac{\sigma_A}{\sigma_B} B . \quad (2)$$

This equation says that given a particular value of B, the *average* value of A is determined (4). This is not to be confused with the sampled population average  $\bar{A}$ . Since the value of A is dependent on B in a linear way, a small change ( $\delta B$ ) in B can be related to a resultant change ( $\delta A$ ) in A. Taking B to represent the set of  $\Sigma K_{FR}$  values and A to represent the ionospheric parameter P, the following very useful expression can be deduced:

$$\frac{\delta P}{P} = \rho(P, \Sigma K_{FR}) \frac{\sigma_P}{P \sigma_{\Sigma K_{FR}}} \delta \Sigma K_{FR} . \quad (3)$$

It will now be of interest to calculate the fractional response of an ionospheric parameter to an impulse in the 3-hourly index  $K_{FR}$ . For an average jump of unity in the 3-hourly  $K_{FR}$  index, the recorded cumulative index  $\Sigma K_{FR}$  must increase by a factor of three. If the 3-hourly index were to jump by an amount  $\delta K_{FR} = 4$ , then  $\delta(\Sigma K_{FR}) = 12$ . Table 9 gives the fractional change in the ionospheric parameters  $N_{F2max}$ ,  $h_{F2max}$ , and  $\tau(600)$  which occurs as the result of a jump  $\delta \Sigma K_{FR} = 12$ . This corresponds to a 9-hr average jump in  $K_{FR}$  of 4. It is noteworthy that the fractions listed in the table are only indicative of fluctuations which would be induced in the average ionosphere by an impulse of magnetic activity at the time-lag index specified.

#### ILLUSTRATION OF MAGNETIC-ACTIVITY RESPONSE

A useful computer program has been constructed from which it is possible to visualize more easily the effect of magnetic activity on the ionosphere. The output of the program is a series of plots corresponding to the shape of the ionospheric electron-density distribution for specified time lags. The plots are not exact; they are idealized Chapman-like functions corresponding to three parameters:  $N_{F2max}$ ,  $h_{F2max}$ , and the scale height H. The parameters  $N_{F2max}$  and  $h_{F2max}$  are measured directly, but H is deduced from the relation

$$\tau = 4.133 H, \quad (4)$$

which is strictly valid only for a Chapman distribution of the form

$$N = N_{F2max} \exp \left( \frac{1 - Z - e^{-Z}}{2} \right), \quad (5)$$

where  $Z = (h - h_{F2max})/H$ . For each month of observation an idealized Chapman distribution is computed having parameters  $\bar{N}_{F2max}$ ,  $\bar{h}_{F2max}$ , and  $\bar{H}$ . The perturbed distribution parameters are given by

Table 9  
 Fractional Change in Ionospheric Parameters for a Jump in  
 in Magnetic Activity of  $\delta\Sigma K_{FR} = 12^*$

Lag (m)	March			April			May		
	$N_{F2max}$	$h_{F2max}$	H, $\tau$	$N_{F2max}$	$h_{F2max}$	H, $\tau$	$N_{F2max}$	$h_{F2max}$	H, $\tau$
2.75	+0.26	+0.06	+0.01	+0.18	+0.15	+0.01	-0.14	+0.16	-0.15
5.75	-0.06	+0.01	+0.02	-0.11	+0.68	-0.04	-0.12	+0.14	-0.13
8.75	-0.33	-0.02	+0.05	-0.29	-0.27	-0.13	-0.14	+0.13	-0.17
11.75	-0.34	-0.01	+0.07	-0.55	-0.13	-0.08	-0.18	+0.14	-0.16
14.75	-0.29	-0.03	+0.04	-0.43	-0.15	-0.11	-0.22	+0.16	-0.16
17.75	-0.23	-0.04	+0.02	-0.41	-0.12	-0.06	-0.30	+0.27	-0.21
20.75	-0.35	-0.07	-0.02	-0.40	-0.12	-0.05	-0.45	+0.26	-0.57
23.75	-0.47	-0.09	-0.02	-0.41	-0.11	-0.06	-0.11	-0.19	-0.23
26.75	-0.46	-0.10	-0.04	-0.29	-0.07	-0.02	-0.05	-0.17	-0.04
29.75	-0.32	-0.07	-0.03	-0.43	-0.09	-0.03	-0.04	-0.12	-0.03
32.75	-0.15	-0.06	-0.04	-0.69	-0.06	-0.13	-0.03	-0.11	-0.03
35.75	-0.09	-0.04	-0.03	-0.62	-0.07	-0.19	-0.04	-0.08	-0.04
38.75	-0.09	-0.04	-0.02	-0.49	-0.05	-0.19	-0.07	-0.07	-0.05
41.75	-0.05	-0.05	-0.02	-0.42	-0.01	-0.18	-0.20	-0.05	-0.08
44.75	-0.07	-0.06	-0.03	-0.53	-0.01	-0.21	-0.15	-0.10	-0.13

\* $\delta\Sigma K_{FR} = 12$  corresponds to a 3-hourly jump in  $K_{FR}$  of 4; this 3-hourly value persists for 9 hr or for three successive 3-hourly periods.

$$N_{F2max} = \overline{N_{F2max}} \left[ \left( \frac{\delta N_{F2max}}{\overline{N_{F2max}}} \right) + 1 \right], \tag{6A}$$

$$h_{F2max} = \overline{h_{F2max}} \left[ \left( \frac{\delta h_{F2max}}{\overline{h_{F2max}}} \right) + 1 \right], \tag{6B}$$

and

$$H_{F2max} = \frac{\overline{\tau}(600)}{4.133} \left[ \left( \frac{\delta \tau(600)}{\overline{\tau}(600)} \right) + 1 \right], \tag{6C}$$

where the fractions within the parentheses were obtained in the previous section. Figures 9-11 show idealized distributions for March-May 1971. The solid curve in each figure is the average monthly distribution, and the dashed curves represent the perturbed distributions.

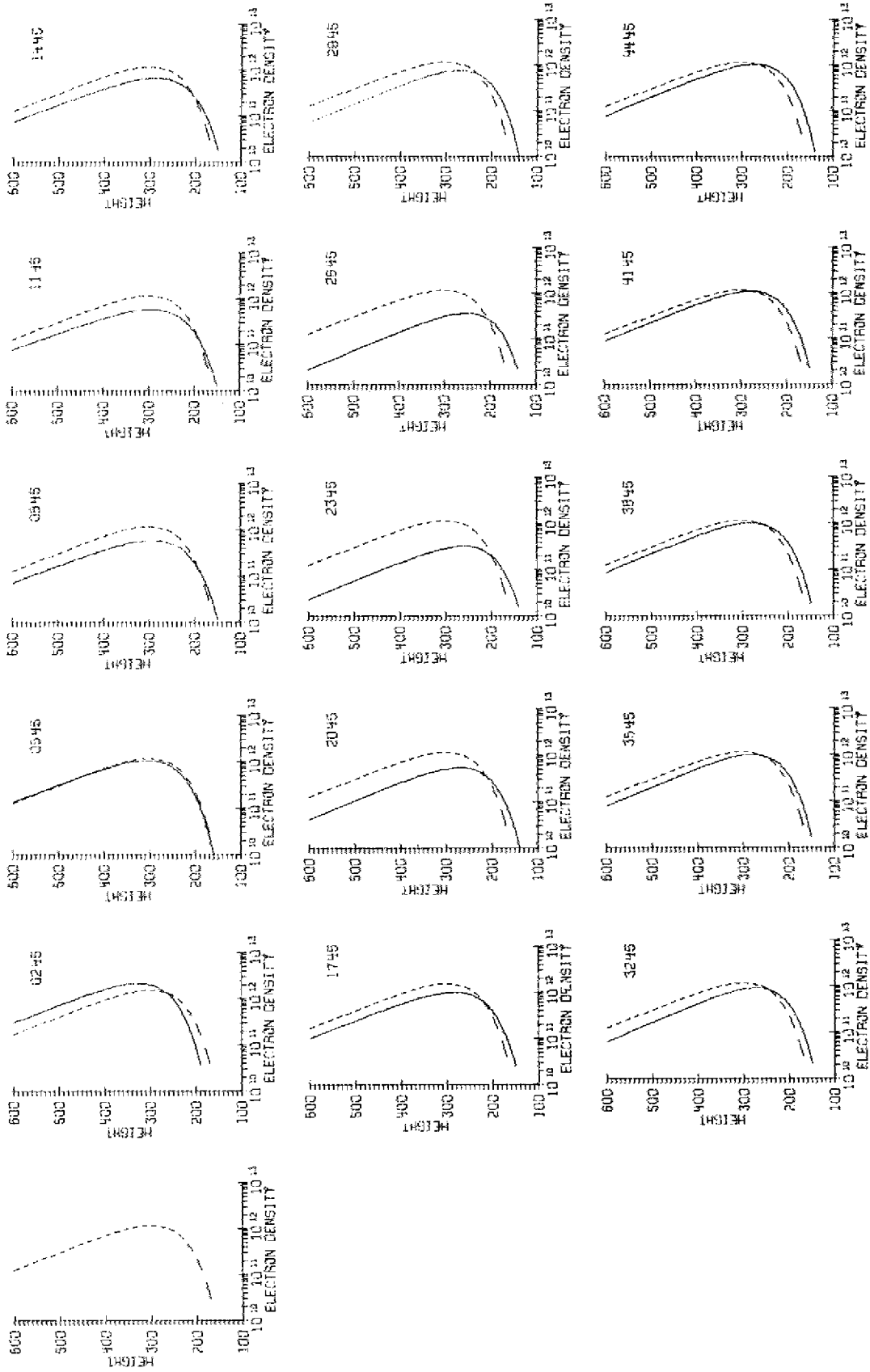


Fig. 9—Idealized response of the ionosphere to magnetic activity as a function of the time lag corresponding to the Thomson scatter observations, March data are depicted. A value of  $\delta \Sigma K_{\text{FIR}} = 18$  was assumed. This corresponds to a severe jump in K<sub>PR</sub> of 6 over a 9-hr period.

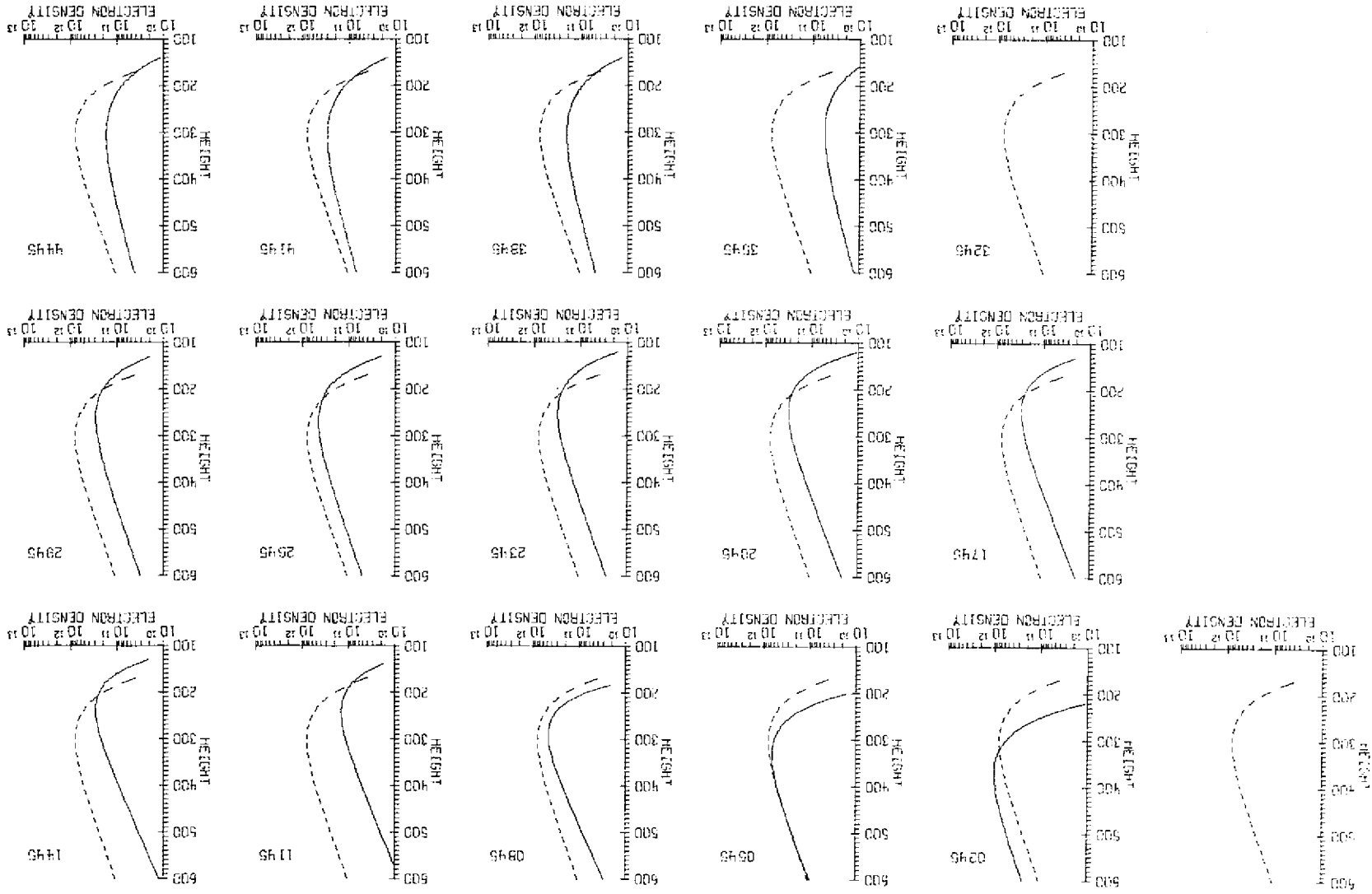


Fig. 10—Idealized response of the ionosphere to magnetic activity as a function of the time lag corresponding to a severe jump in Kp of 6 over a 9-hr period. A value of  $\delta KpR = 18$  was assumed. This corresponds to the Thomson scatter observations. April data are depicted.

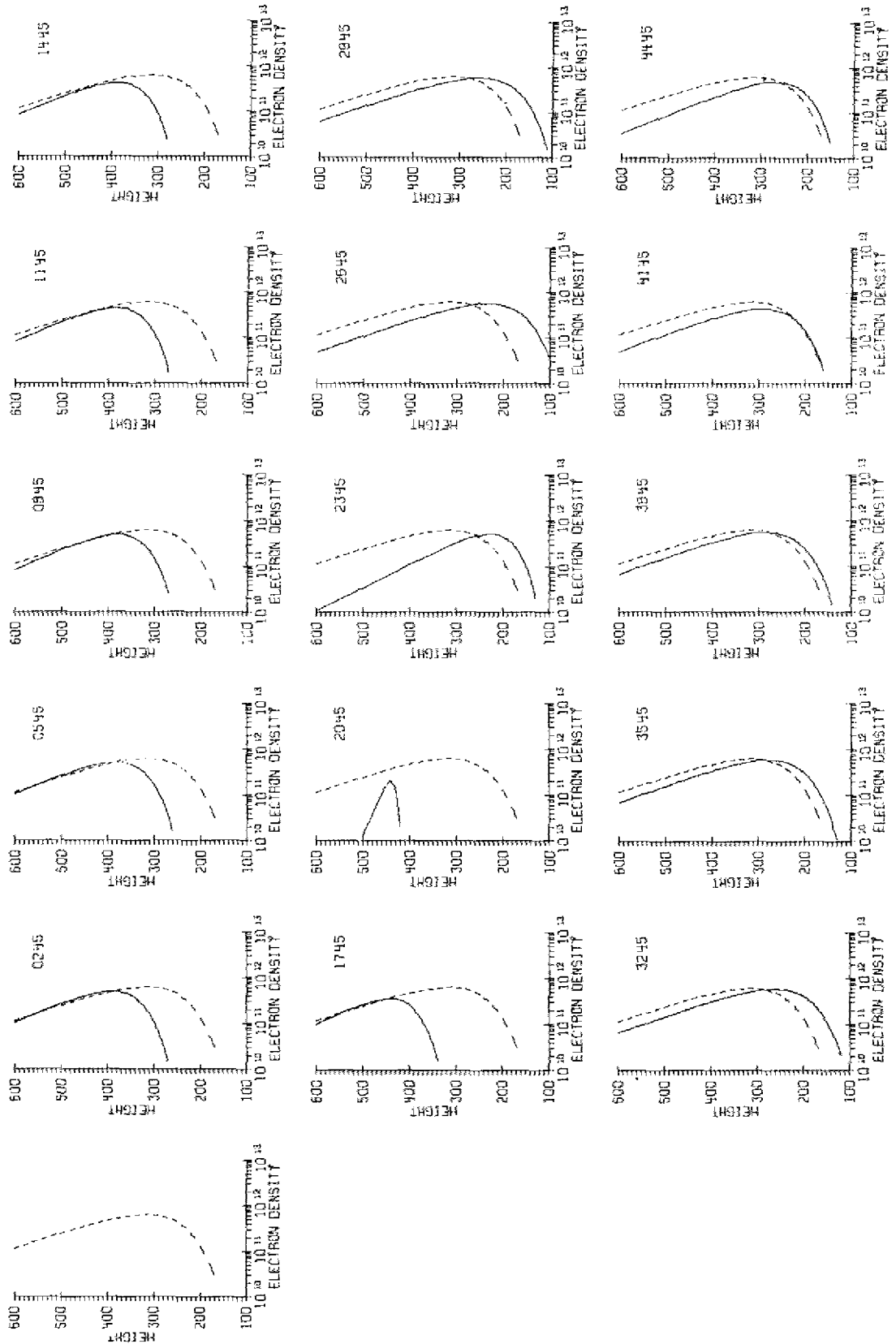


Fig. 11—Idealized response of the ionosphere to magnetic activity as a function of the time lag corresponding to the Thomson scatter observations. May data are depicted. A value of  $\delta\Sigma K_{F2} = 18$  was assumed. This corresponds to a severe jump in K<sub>F2</sub> of 6 over a 9-hr period.

## DISCUSSION

It has been known for some time that magnetic storms produce an effect on the concentration of electrons in the ionosphere. The general behavior is one in which the variation in electron density is an increase followed by a decrease. The negative main phase of the magnetic storm is normally associated with a drop in the total electron content. It has been shown by Jacchia (5) and Newton et al. (6) that the neutral species are heated by magnetic activity. It is anticipated that this heating and the related turbulence produced in the atmosphere will increase the height at which diffusive separation appears, thus increasing the electron loss rate (7). On the other hand, Taylor (8) has observed large decreases in electron production during the negative phase of magnetic storms—a fact which suggests that a decrease in the rate of electron production may be at least as important as an increase in the electron loss rate. The first report of a large-scale enhancement in the total electron content during the initial positive phase of a magnetic storm was made by Goodman (9) using synchronous-satellite data obtained in 1967. The effect has been studied rather exhaustively by Papagiannis et al. (10) who suggest that positive storm effects are primarily a dusk phenomenon. Goodman (9) has suggested that electrodynamic forces may play a role in the enhancement of total content, and this possibility has been given some support by Evans (11). Recently Jones (12) and Jones and Rishbeth (13) have studied the storm-time variation of the F2-layer electron concentration and the possible origins of the variation. They claim that the two effects are produced by competing processes and that the positive effect is produced by storm-induced changes in the thermospheric wind pattern. They also suggest that an increase in the equatorward neutral wind will drive the F2 layer to greater heights, thus increasing the electron concentration, since the loss coefficient is an exponentially decreasing function of height. (Of course, the neutrals only move horizontally, but their motion imparts an effectively upward movement to the ions because of the presence of the magnetic field.)

The present data were obtained during periods of generally quiet geomagnetic activity. Nevertheless, one minor geomagnetic storm did occur during May. The effects of this storm may be seen by comparing Figs. A19-A26 in the appendix. The primary thrust of this study, however, is directed toward the effect of low-level magnetic activity on the ionosphere. The depletion in electron concentration following a moderate excursion of magnetic activity is illustrated in Fig. 12. An approximate 30% drop in the F2 peak electron density occurred on April 22 following an increase in magnetic activity on April 21. In addition the F2 layer height decreased substantially between the two days. It is anticipated that the phenomena responsible for this behavior are active for all degrees of magnetic activity. Indeed, the results of an analysis of the Thomson scatter data obtained at Randle Cliff are consistent with the notion of a depletion in electron concentration at some time following a small impulse of magnetic activity. This electron-content depletion is controlled by a depletion of the F2 maximum density, and this effect is generally greatest whenever the magnetic activity precedes the profile measurement by  $\approx 16$  hr, on the average. Such a lag is also characteristic of the ionospheric response to large magnetic storms. The immediate response of the ionosphere (the response for small lag times) is a slight enhancement in the total content during March and April and a decay in May. The March-April behavior is characteristic of the initial buildup of electron content which occurs during the positive phase of many magnetic storms. Even during May the amount of initial electron-content decay was less at the early lag times than during later times ( $\approx 15$  hr).

Evidently two competing processes are in progress, with the positive-phase process occurring first and the negative-phase process occurring somewhat later. It is possible that the negative-phase process is broader during May and adds a negative bias to the initial positive response. During March and April, the negative phases are not as broad.

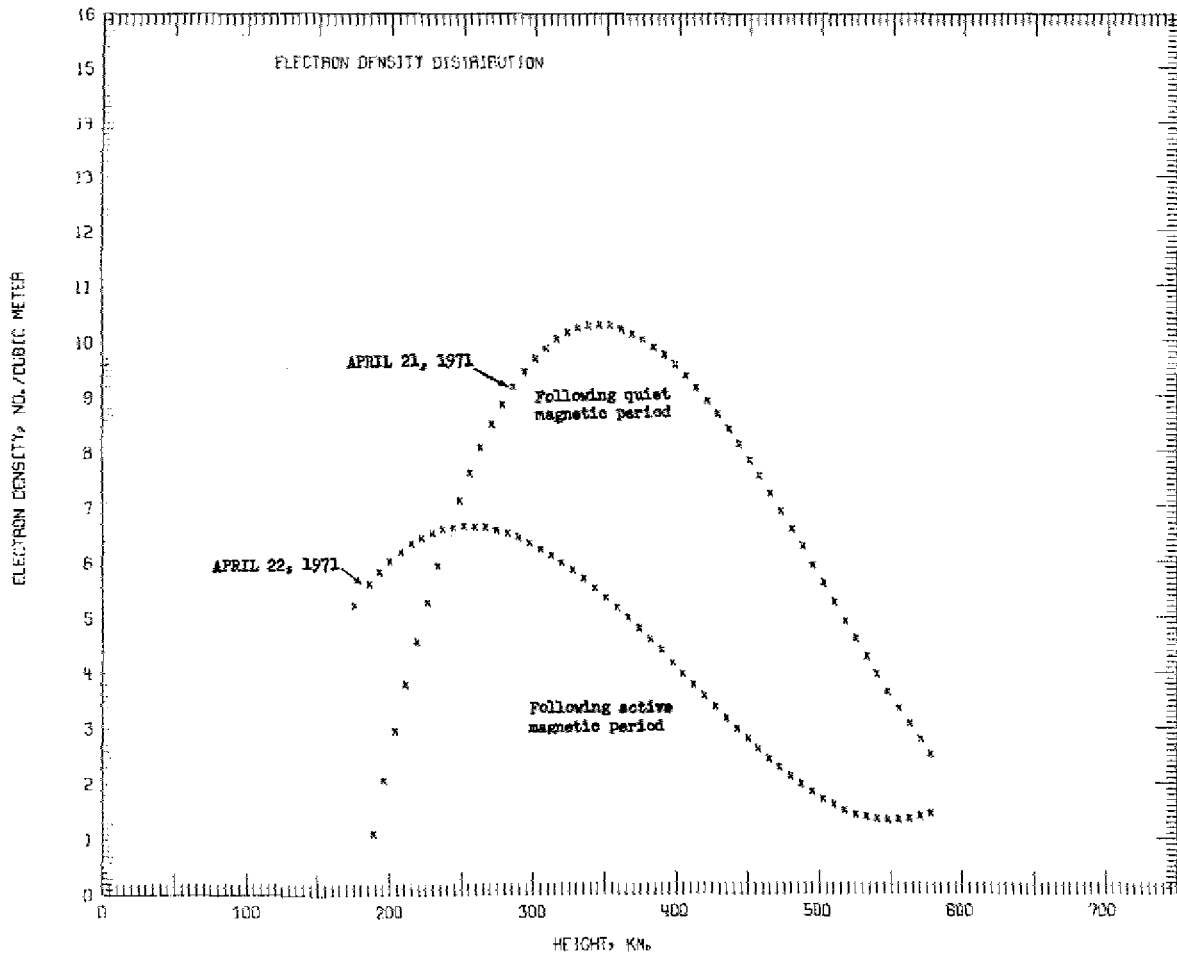


Fig. 12—The response of the ionosphere to magnetic activity. The magnetic activity increased on April 21, causing a diminution in the electron content on April 22. Also, the F2 maximum height dropped substantially on April 22.

It is emphasized that the results previously presented in the section on the modification of parameters assume normally distributed random variables. It is anticipated that the variables ( $K_{FR}$  and the ionospheric parameters  $N_{F2max}$ ,  $h_{F2max}$ ,  $C(600)$ , and  $\tau(600)$ ) will be so distributed in nature. Unfortunately the populations are sampled so seldom for each lag interval (between eight and ten times) that it is not possible to establish this fact with any statistical significance. Naturally, by combining the runs from all three months, it should be possible to conduct significant chi-square tests to determine the goodness of fit for each distribution. Unfortunately such a combination of the three months is not appropriate, due to the rather obvious seasonal dependence in the data. A possible approach to solving this problem would be to remove the seasonal bias prior to processing. This

approach has not been attempted as of this writing. It will be carried out eventually, however, and the results will be contained in a final report.

## SUMMARY

Radar Thomson scatter observations of the midday ionosphere were made during March, April, and May 1971. From these observations the following F-region parameters were deduced: the F-region peak density  $N_{F2max}$ , the F2 maximum height  $h_{F2max}$ , the total content below 600 km  $C(600)$ , and the equivalent slab thickness  $\tau(600)$ . The average monthly electron population decreased between March and May, as expected, since the equinoctial ionosphere is more dense than the summer ionosphere at midlatitudes. It was found that the total content is strongly controlled by the peak F-region density for all three months. In addition, fluctuations in the F2 maximum height were positively correlated with fluctuations in the  $N_{F2max}$ ,  $C(600)$ , and  $\tau(600)$  during March and April; the converse was true in May. During May there was almost no correlation between the parameters  $N_{F2max}$  and  $\tau(600)$ , however, during March and April the correlation was negative. It was also found that  $C(600)$  and  $\tau(600)$  were almost independent during the first two months, but during May they were positively correlated. It is suggested that the differences in the March-April and the May results may be partially explained by the differences in the character of the magnetic activity during the two periods.

An examination of the time lag between measurements of the Fredericksburg  $K_{FR}$  index and the Thomson scatter observations leads to the construction of crosscorrelation functions between the degree of magnetic activity and various ionospheric parameters. Assuming a gaussian distribution of the random variables, the average ionospheric response to an impulse of magnetic activity has been deduced. The general behavior is one in which the F2 maximum height increases initially in proportion to the amount of magnetic activity, subsequently decreases, and eventually returns to its equilibrium value. It is found also, that the F2 maximum density and the total content decrease with increasing lag time, the greatest diminution occurring at  $\approx 16$  hr, on the average. The F-region scale height, on the basis of an idealized Chapman profile, displays no consistent behavior for the three months.

Future emphasis will be directed toward removing the seasonal dependence from the observations and constructing crosscorrelation functions between the various ionospheric parameters and the magnetic A indices or their equivalents. The A indices are more linearly related to magnetic activity than are the K indices which were used in the present analysis.

## REFERENCES

1. J. M. Goodman and M. W. Lehman, "Midday Electron Density Profiles over Randle Cliff for March 1971," NRL Memorandum Report 2344, Sept. 1971.
2. J. M. Goodman, "A VHF Thomson Scatter Radar Study of the Midlatitude Ionosphere Using the Faraday Effect," NRL Report 7221, Apr. 1971.

3. J. M. Goodman, "Radar Thomson Scatter Profiles of the Ionospheric Electron Density Observed Near Washington, D.C., During March, April, May 1971," NRL Technical Memorandum 5370-100, Nov. 1971.
  4. J. V. Uspensky, *Introduction to Mathematical Probability*, McGraw-Hill, New York, 1937, p. 314.
  5. L. G. Jacchia, "Influence of Solar Activity in the Earth's Upper Atmosphere," *Planetary Space Sci.* **12**, 355 (1964).
  6. G. P. Newton, R. Horowitz, and W. Preister, "Atmospheric Density and Temperature Variations from the Explorer XVII Satellite and a Further Comparison with Satellite Drag," *Planetary Space Sci.* **13**, 599 (1965).
  7. J. E. Titheridge and M. K. Andres, "Changes in the Topside Ionosphere During a Large Magnetic Storm," *Planetary Space Sci.* **15**, 1157 (1967).
  8. G. N. Taylor, "Measurement of the Electron Content of the Ionosphere During Some Magnetically Disturbed Periods in Winter," *J. Atmos. Terr. Phys.* **27**, 735 (1968).
  9. J. M. Goodman, "Some Measurements of Electron Content Enhancements Associated with Magnetic Storms," *Planetary Space Sci.* **16**, 951 (1968).
  10. M. D. Papagiannis, M. Mendillo, and J. A. Klobuchar, "Simultaneous Storm-Time Increases of the Ionospheric Total Electron Content and the Geomagnetic Field in the Dusk Sector," *Planetary Space Sci.* **19**, 503 (1971).
  11. J. V. Evans, "Incoherent Scatter Observations of F-Region Storm Effects," 1970 Spring Meeting of URSI, Washington, D.C.
  12. K. L. Jones, "Storm-Time Variation of the F2 Layer Electron Concentration," *J. Atmos. Terr. Phys.* **33**, 379 (1971).
  13. K. L. Jones and H. J. Rishbeth, "The Origin of Storm Increases of Midlatitude F-Layer Electron Concentration," *J. Atmos. Terr. Phys.* **33**, 391 (1971).
-

**APPENDIX**  
**Electron-Density Distributions for March, April, and May 1971**

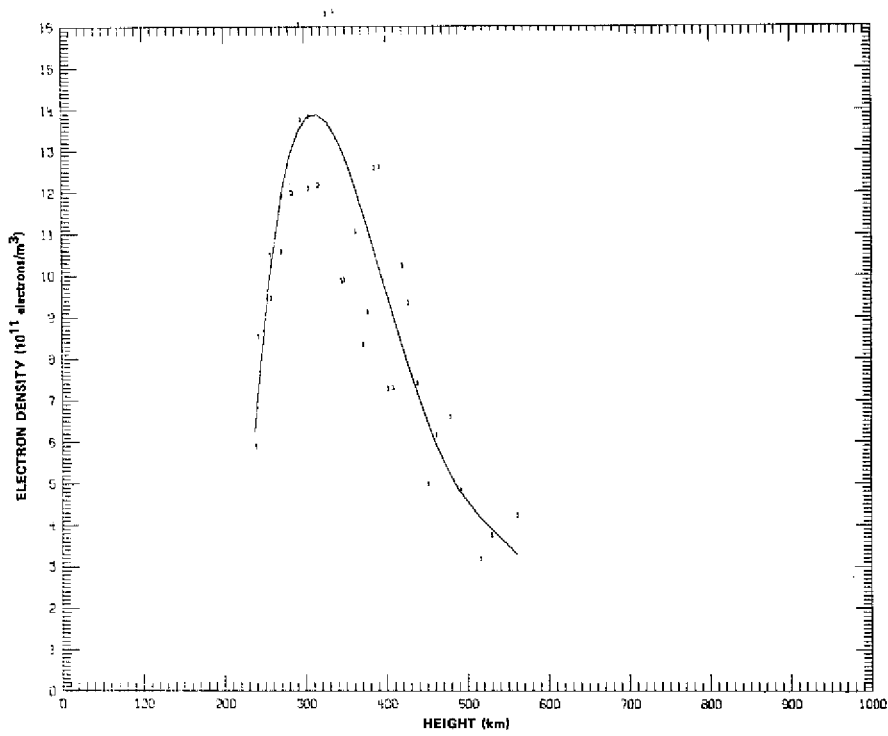


**Fig. A1—March 12, 1971**

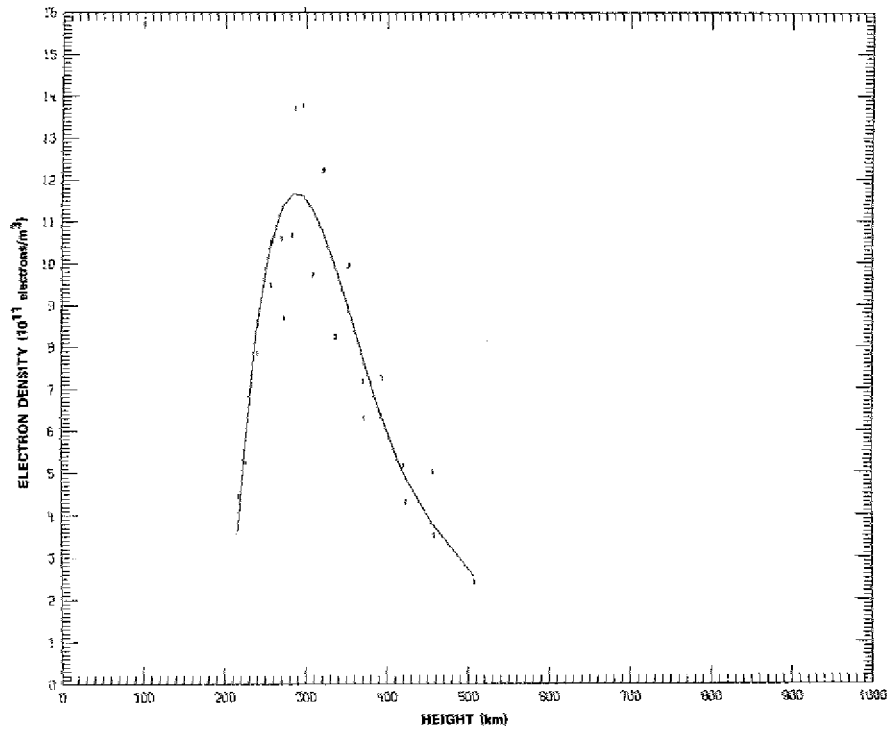


Fig. A2—March 15, 1971

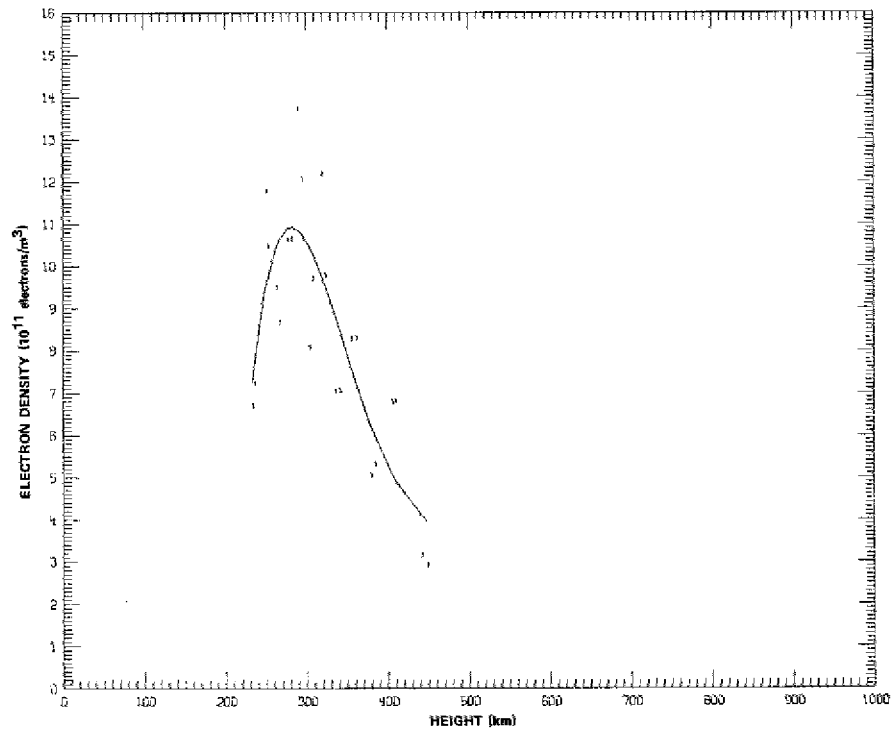


Fig. A3—March 14, 1971

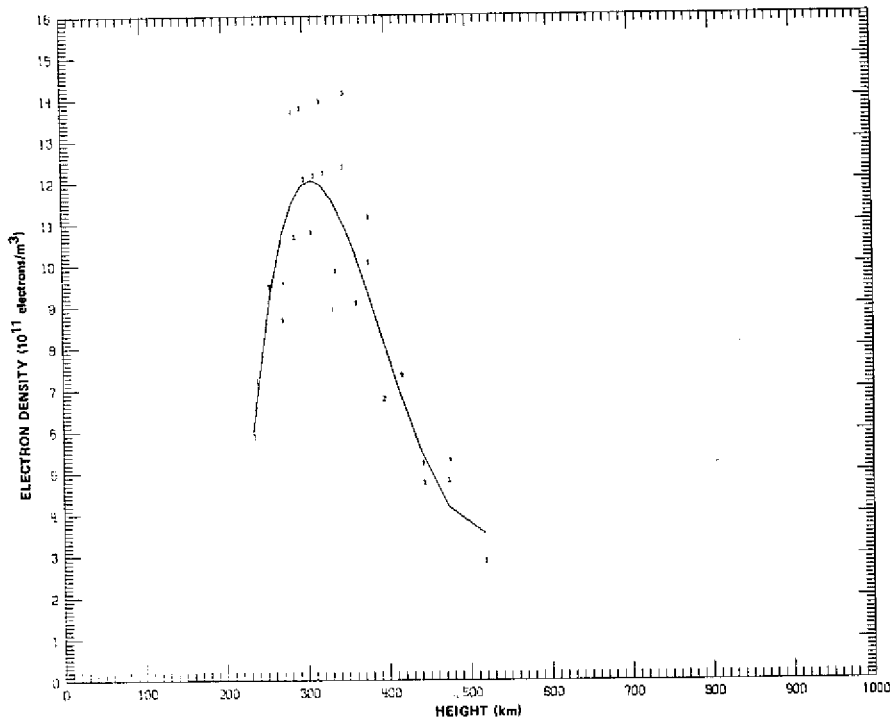


Fig. A4—March 17, 1971

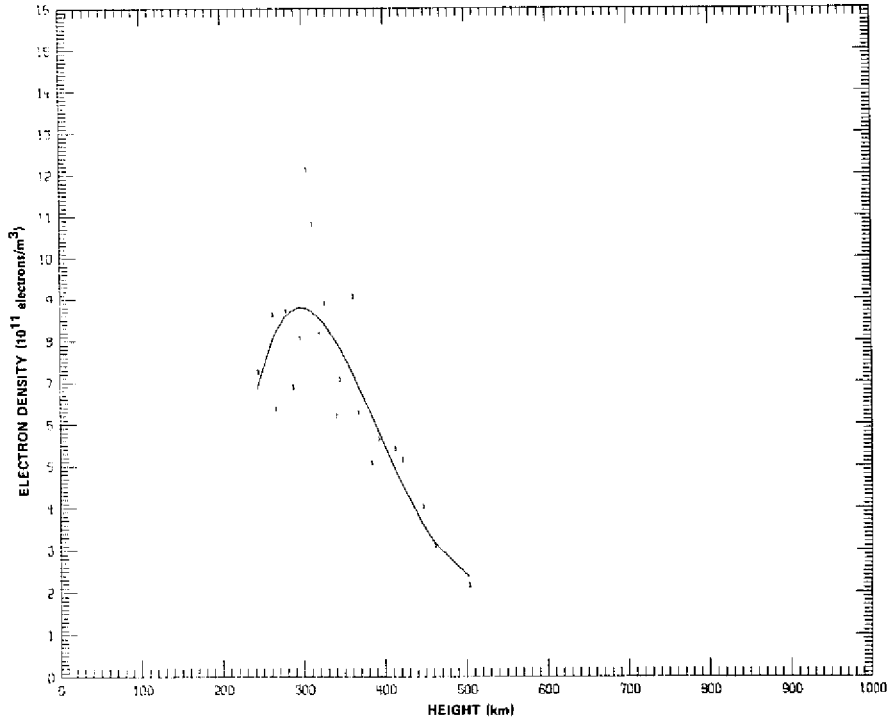


Fig. A5—March 18, 1971

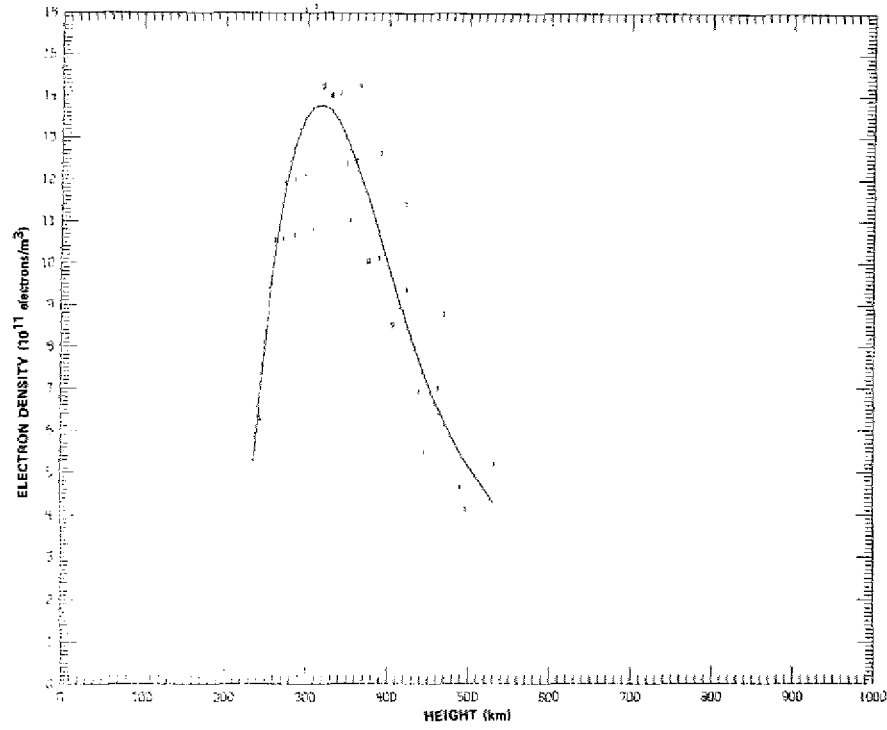


Fig. A6—March 19, 1971

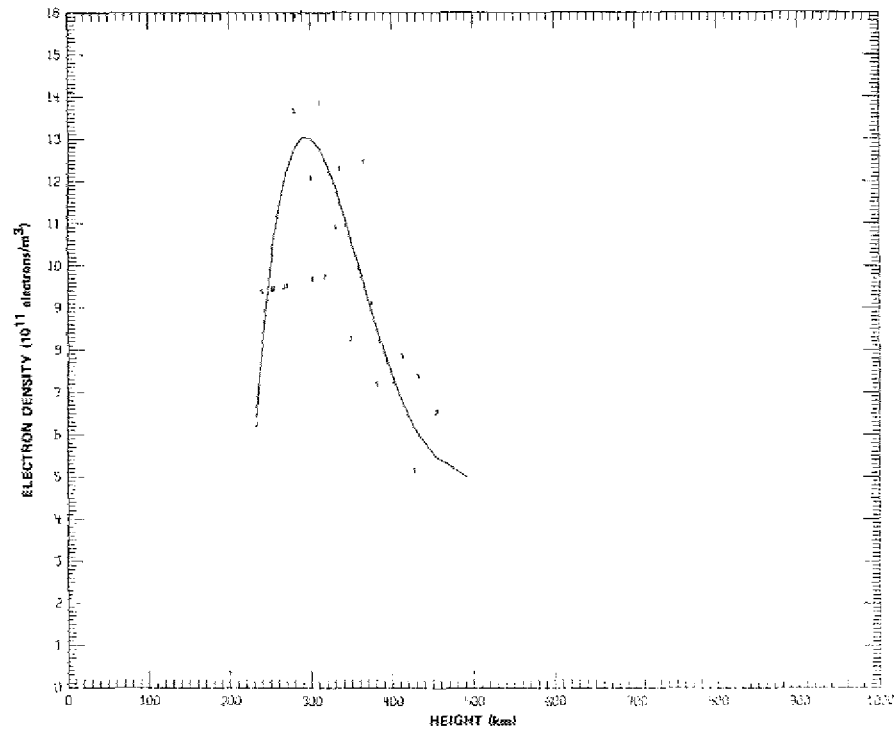


Fig. A7—March 22, 1971

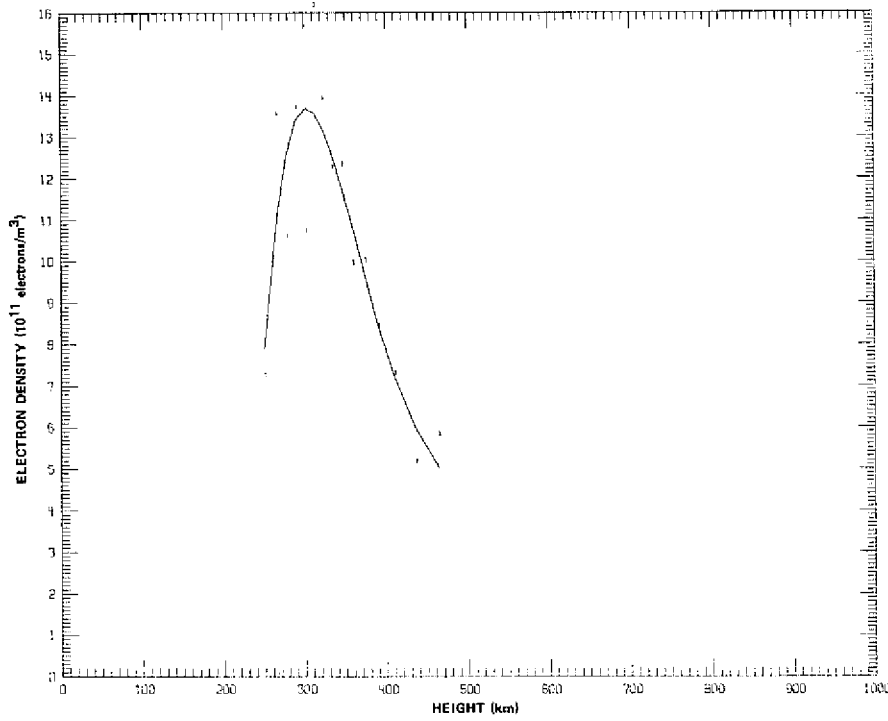


Fig. A8—March 23, 1971

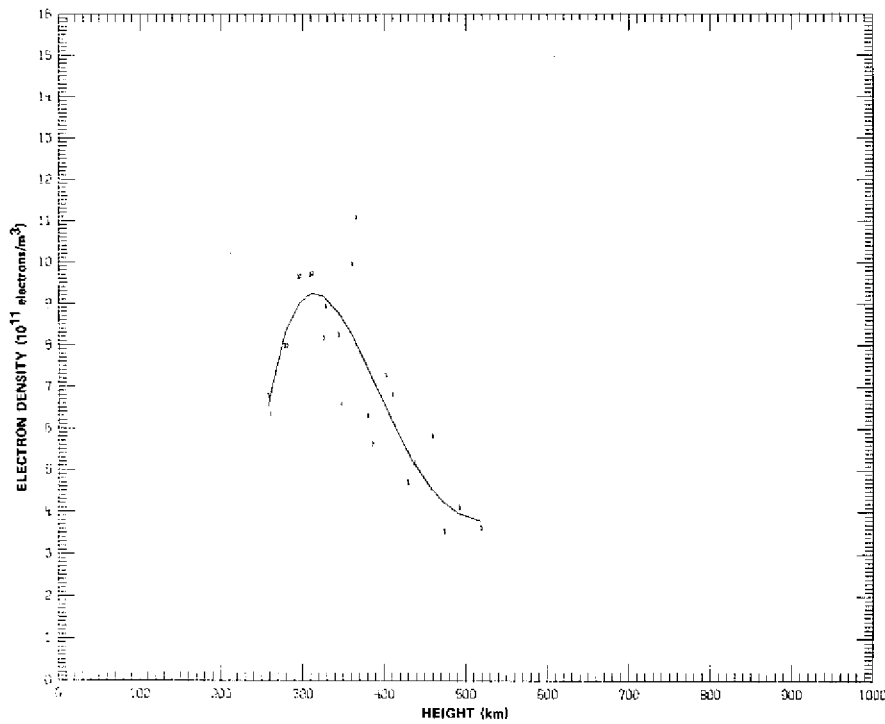


Fig. A9—March 24, 1971

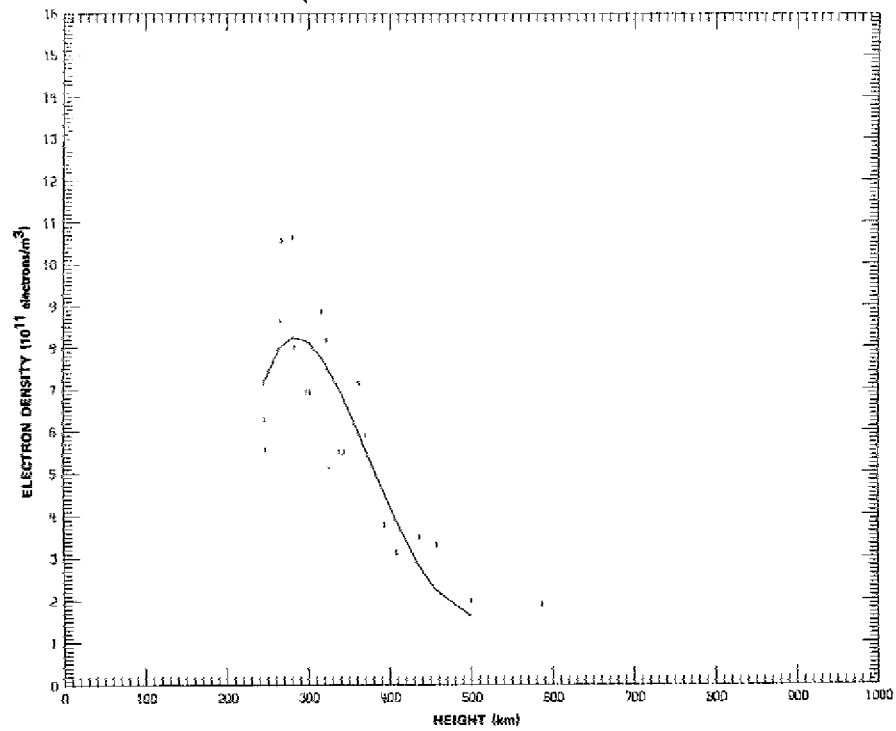


Fig. A10—March 25, 1971

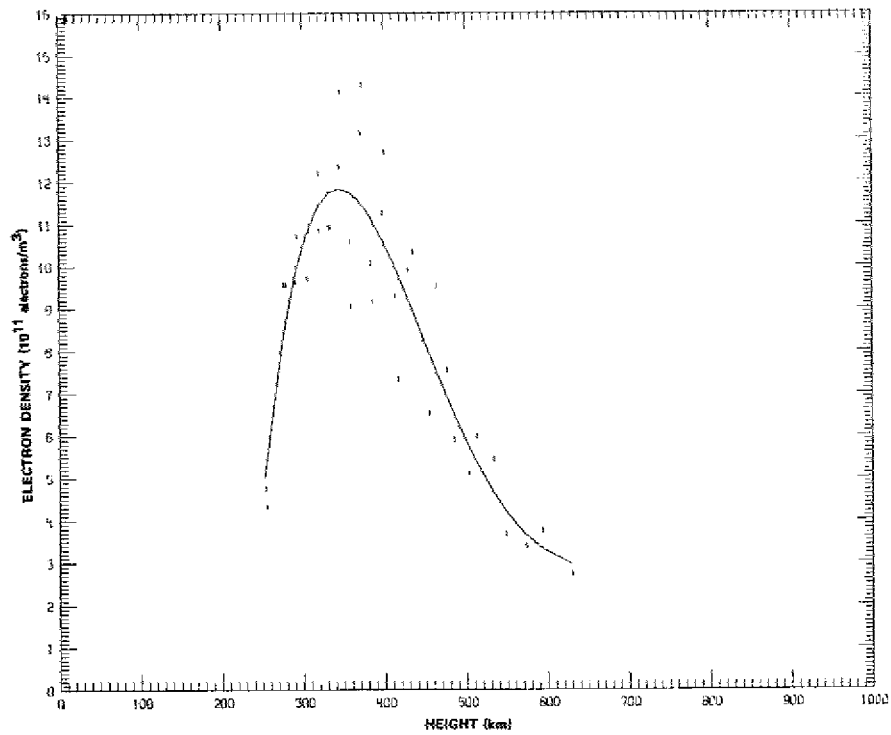


Fig. A11—April 21, 1971

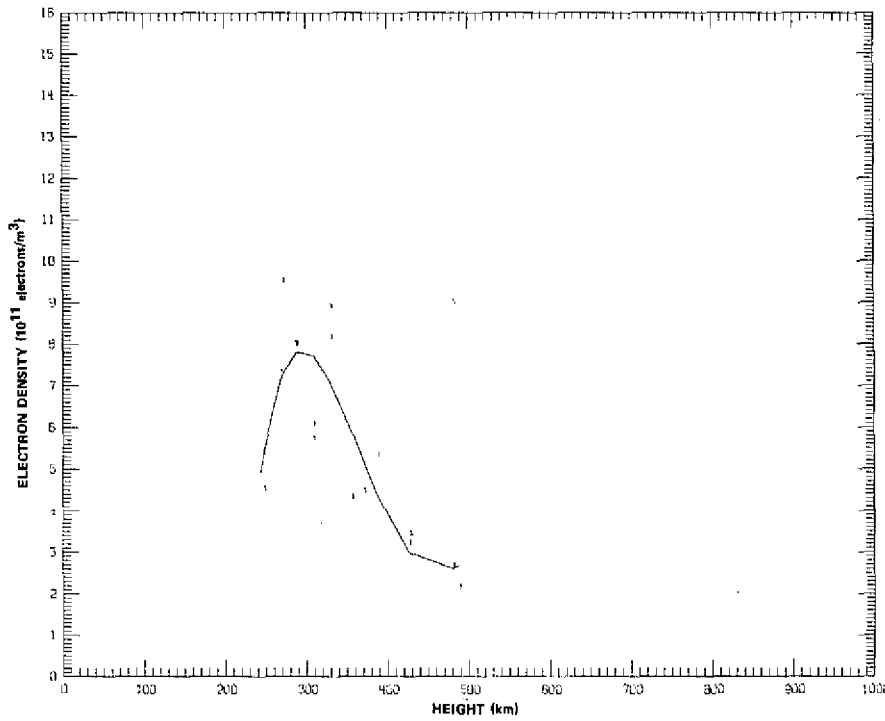


Fig. A12—April 22, 1971

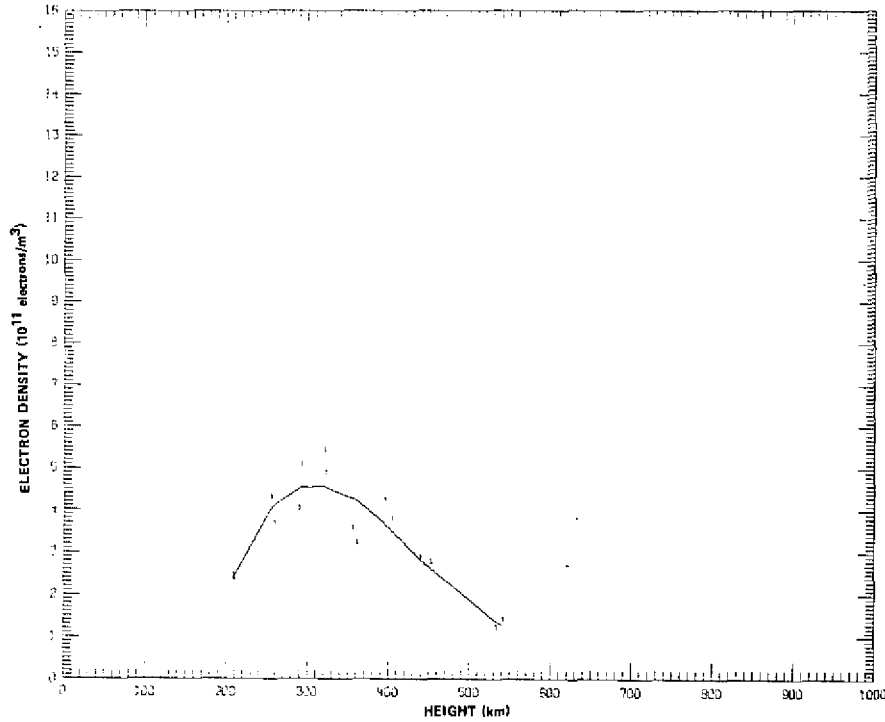


Fig. A13—April 23, 1971

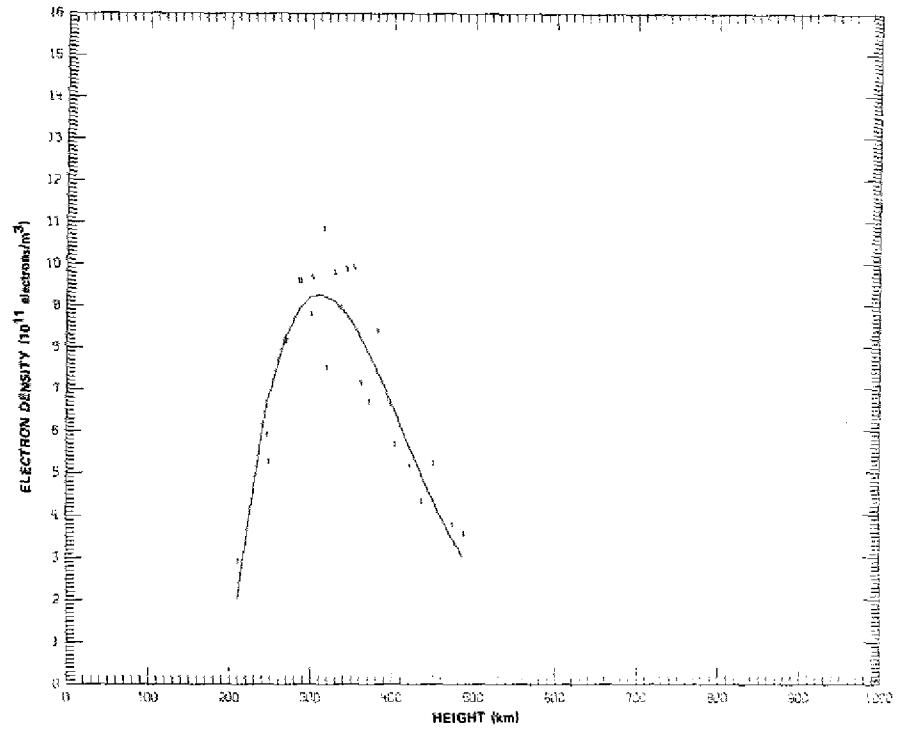


Fig. A14—April 26, 1971

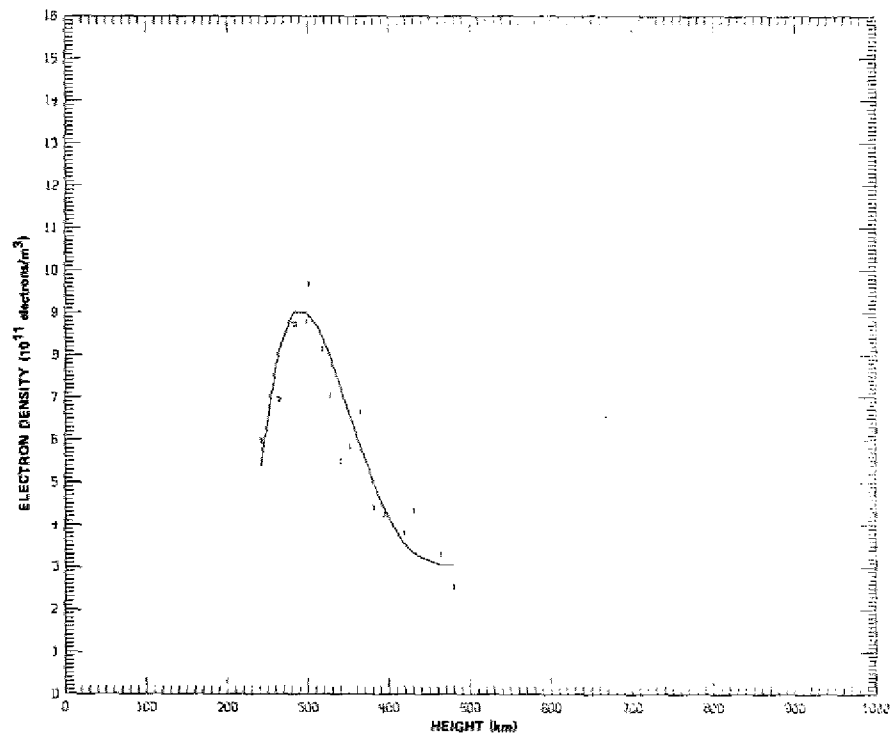


Fig. A15—April 27, 1971

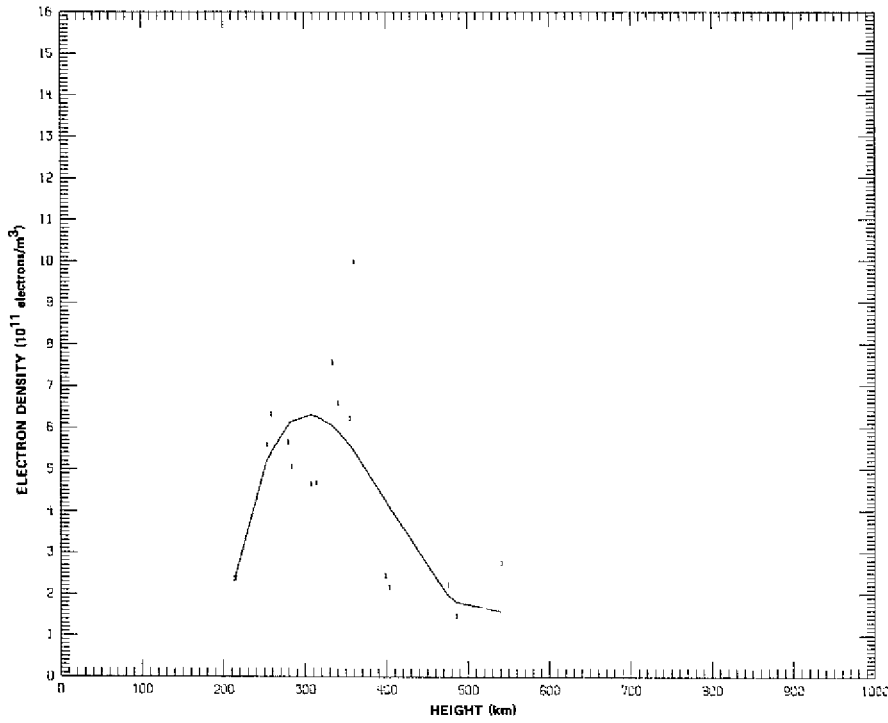


Fig. A16—April 28, 1971

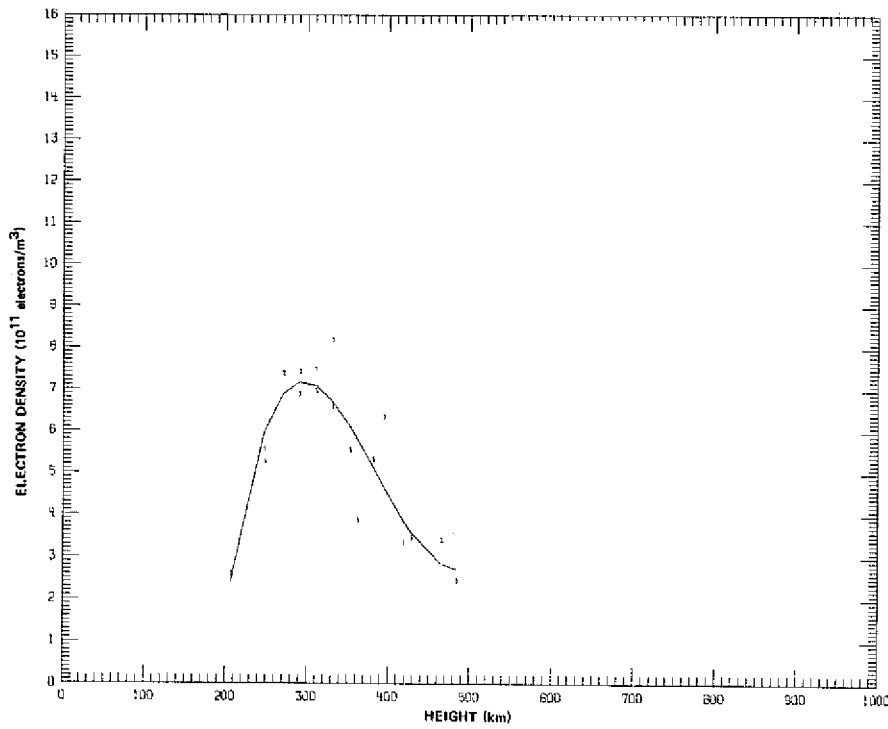


Fig. A17—April 29, 1971

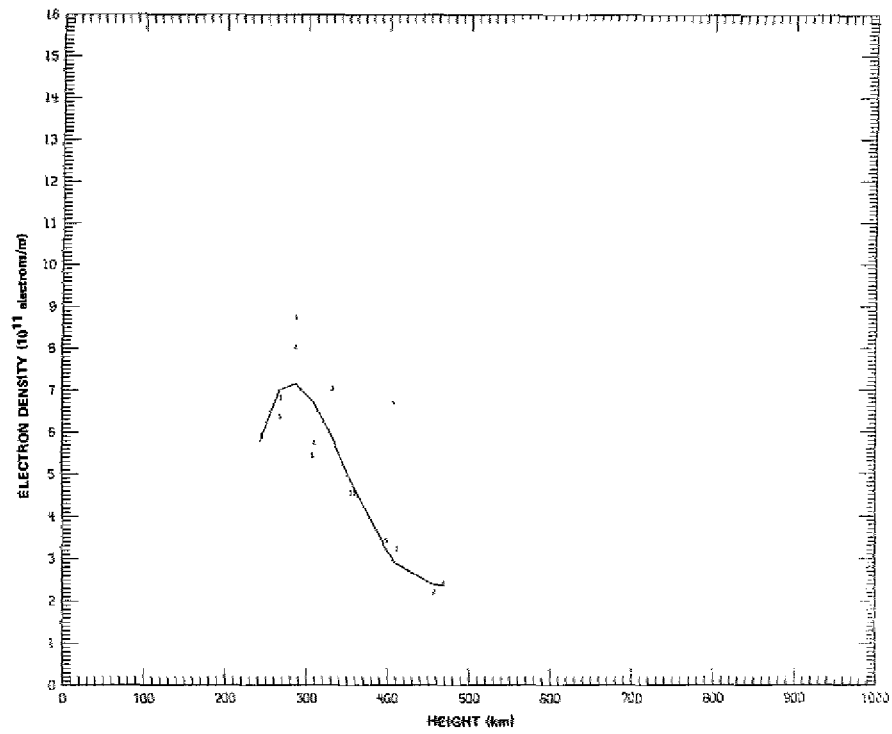


Fig. A18—April 30, 1971

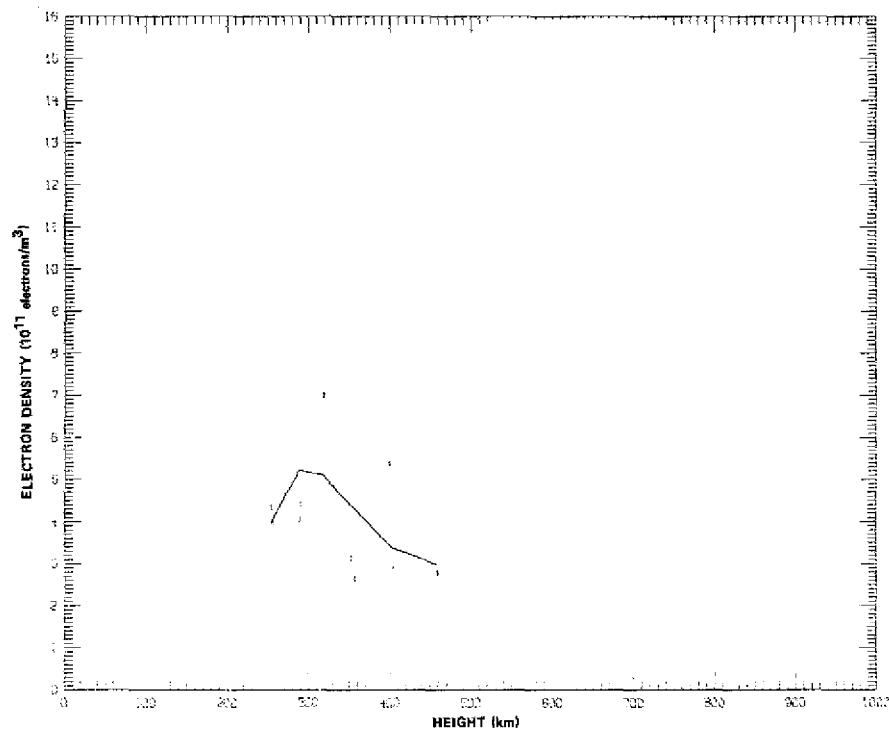


Fig. A19—May 11, 1971

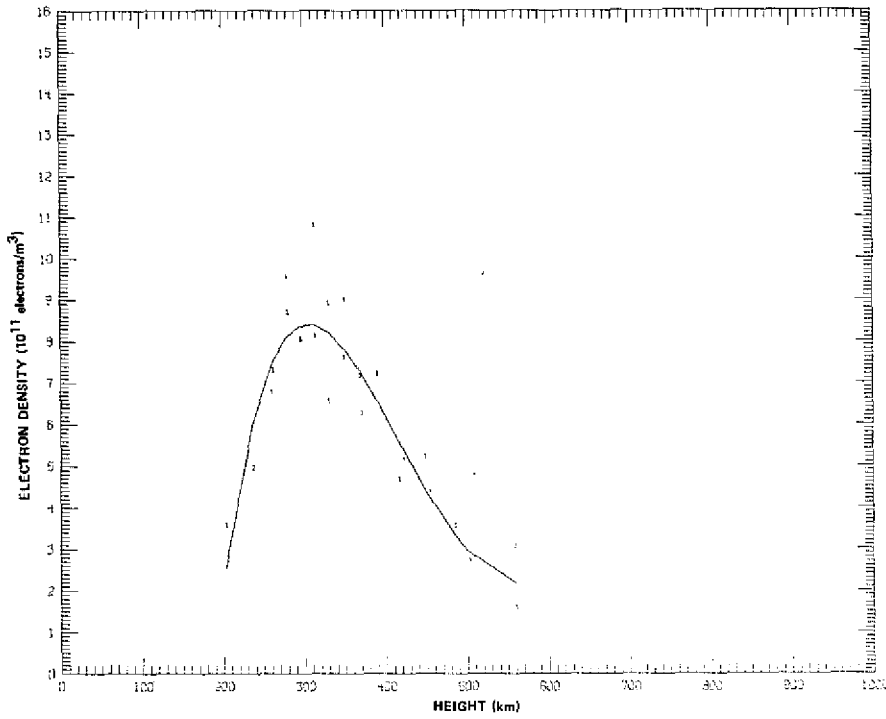


Fig. A20—May 12, 1971

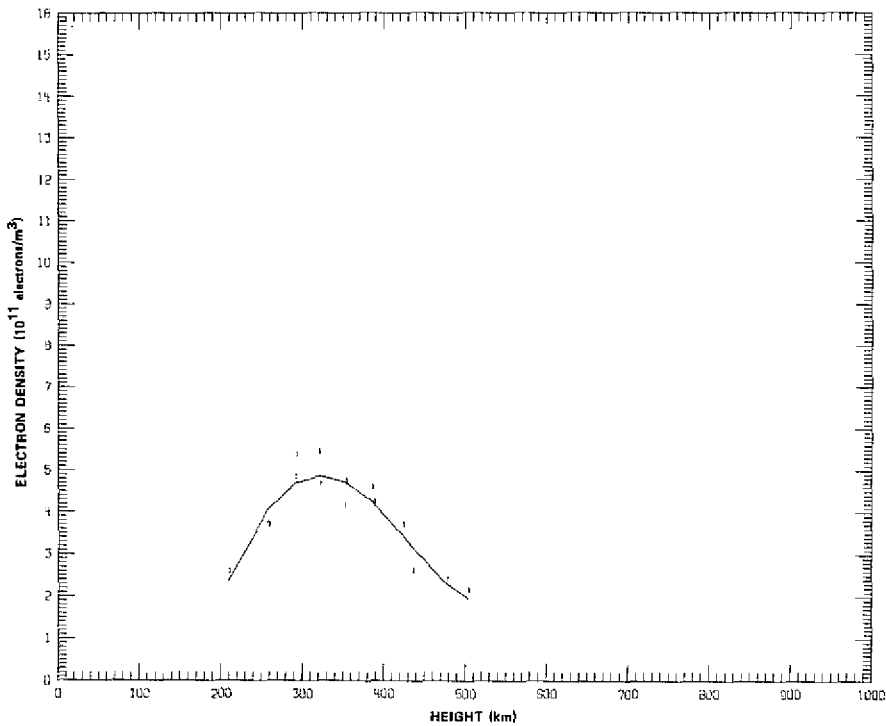


Fig. A21—May 13, 1971

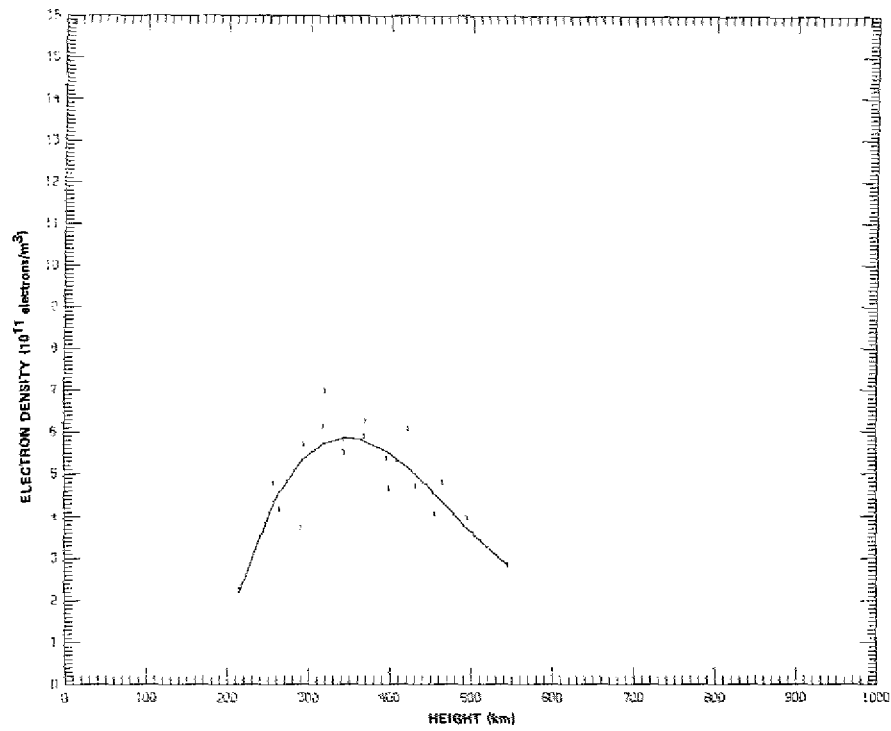


Fig. A22—May 14, 1971

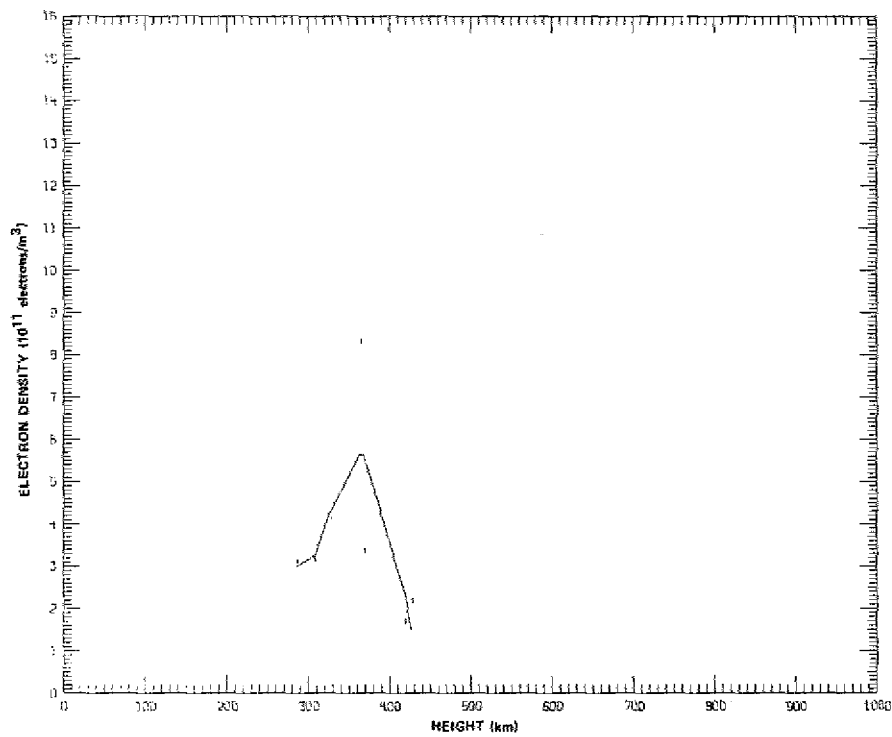


Fig. A23—May 17, 1971

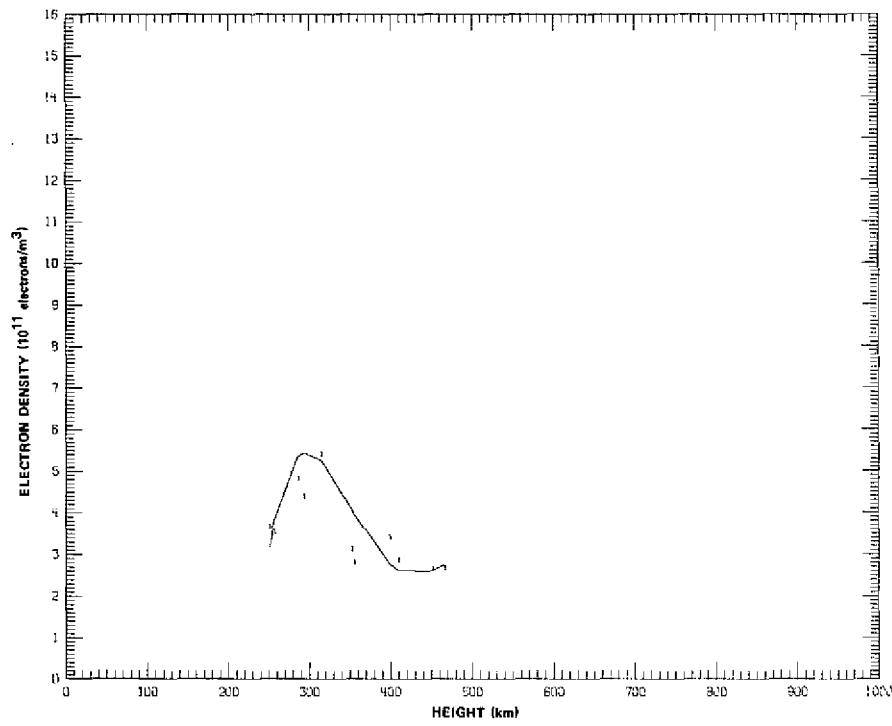


Fig. A24—May 19, 1971

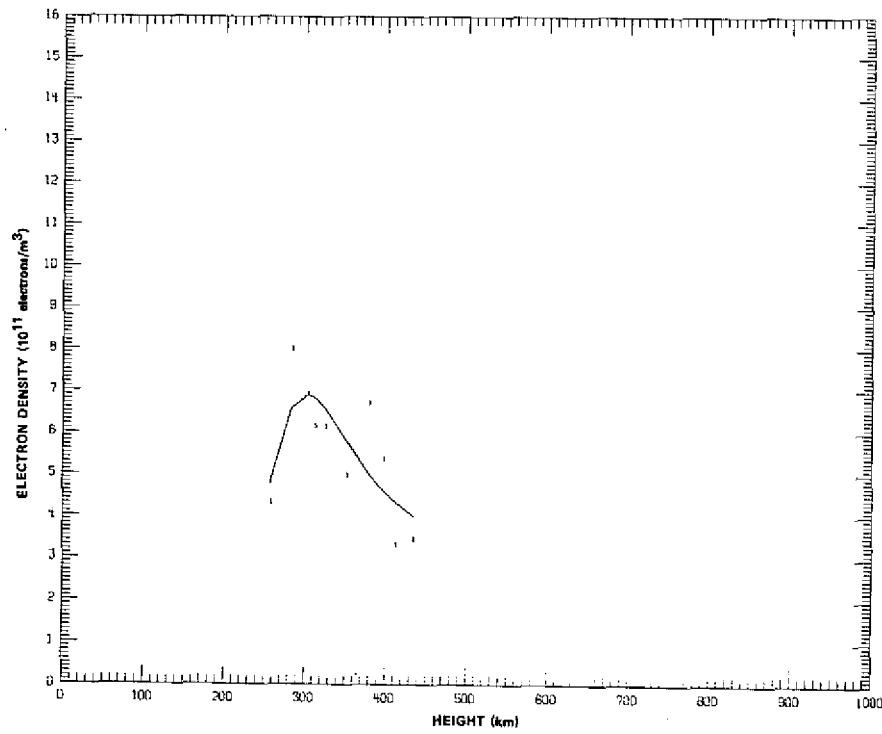


Fig. A25—May 20, 1971

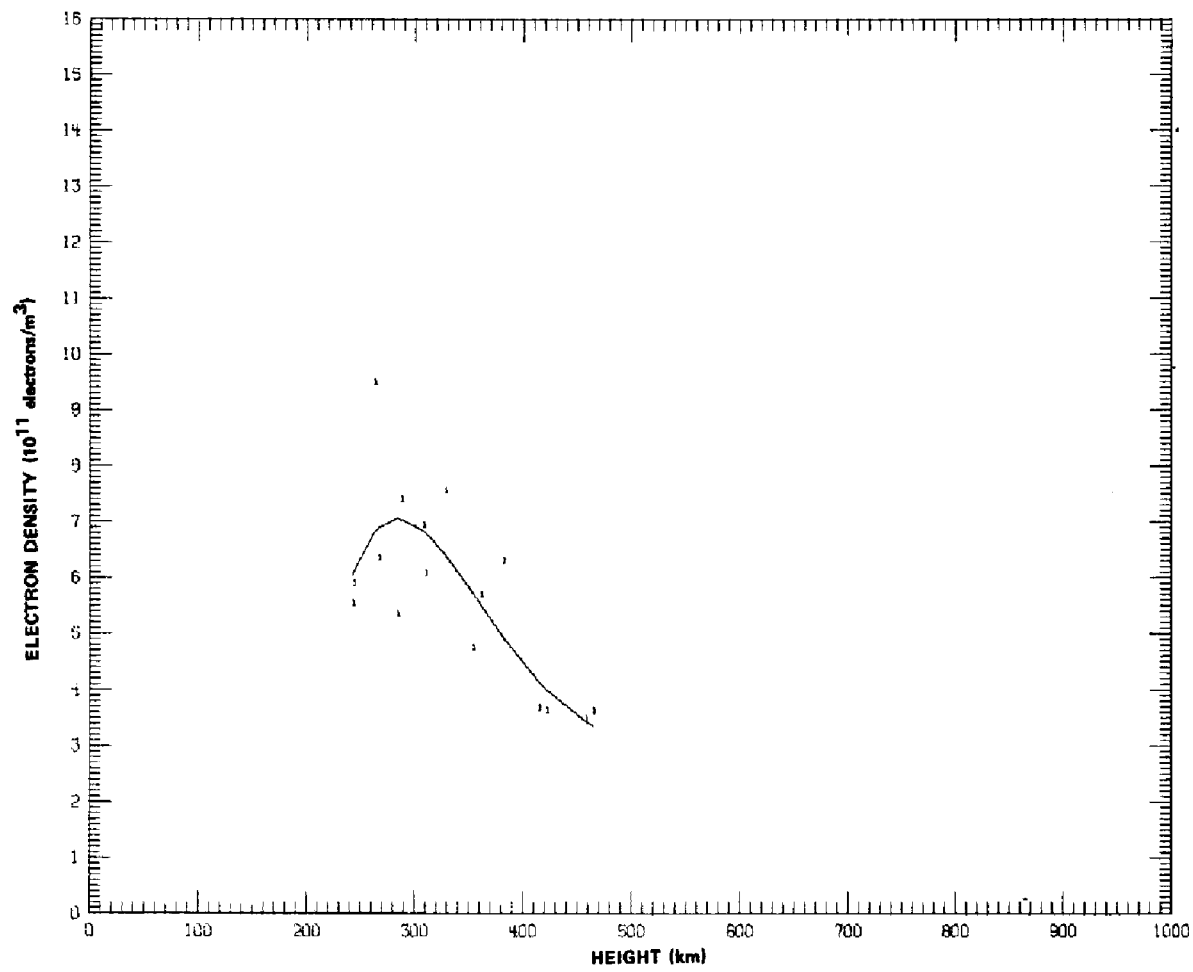


Fig. A26—May 21, 1971